

EXPLORATORY AUDITORY EEG-ERP PARADIGM FOR DOC PATIENTS

DEVELOPING AN ERP PARADIGM TO ASSESS CONCEPTUAL PROCESSING IN
DOC PATIENTS: A PROOF OF PRINCIPLE STUDY

By NETRI PAJANKAR, B.Sc.

A Masters Thesis Submitted to the School of Graduate Studies in Partial Fulfillment of
the Requirements for the Degree Master of Science McMaster University

© Copyright by Netri Pajankar, August 2022

McMaster University MASTER OF SCIENCE (2022) Hamilton, Ontario (Neuroscience)

TITLE: Developing an ERP Paradigm to Assess Conceptual Processing in DOC

Patients: A Proof of Principle Study

AUTHOR: Netri Pajankar, B.Sc. (McMaster University)

SUPERVISOR: John Connolly

NUMBER OF PAGES: xiii, 68

Lay Abstract

Severe brain damage can sometimes result in a set of neurological conditions called Disorders of Consciousness (DOC). These patients are often misdiagnosed due to clinical protocols relying on observation of visible signs of brain function and awareness. A brain imaging technique called electroencephalography (EEG) records electrical brain activity using metal discs or electrodes attached to the scalp. This can provide information about various kinds of cognitive and sensory activity. This study aims to investigate whether spoken words and environmental sounds can induce brain activity related to understanding meaning in healthy participants, and ultimately, in DOC patients.

Abstract

Severe acquired brain damage can sometimes result in a set of conditions resulting in altered states of consciousness, called Disorders of Consciousness (DOC). Event-related potentials (ERPs) extracted from electroencephalography (EEG) have proven to be a reliable neuroimaging method to accurately diagnose and predict the outcome of patients with DOC. The N400 component indicates higher order cognitive activity associated with processing, including language, music, and environmental sounds. An increased N400 amplitude has mainly been observed in response to sentence and word priming paradigms, mostly from healthy and native speakers of the language. Stimuli like sentences can tax working memory, which can cause misinterpretation of a patient's condition as reflecting a language dysfunction when, in fact, the problem is about memory. Environmental sounds, or sounds related to common events, encode conceptual meanings similar to language and could be easier for such patients to comprehend. This study introduces a unimodal auditory priming paradigm with environmental sounds and spoken words to investigate if significant N400 activity could be elicited in a sample of 18 healthy participants and one DOC patient. ERP components (N400, N100 and P200) were extracted and averaged across 18 participants, as well as collected individually from each participant and one patient. The environmental sounds were paired with conceptually congruent and incongruent words. Comparisons of amplitude and latency were made between

congruent and incongruent conditions. Statistical analysis indicated that the N400 amplitude peak in response to incongruent sound-word pairs was significantly higher than the responses to the congruent sound-word pairs across the grand average of 18 participants and for each individual participant as well. Significant differences for the amplitude and latency of N100 and P200, components that indicate auditory processing were seen across the average of 18 participants. The DOC patient showed a possible N400 effect upon visual inspection. Further testing of this paradigm with more non-communicative patients with neurological dysfunction is required to determine the utility of this priming paradigm in clinical protocol for diagnostic and prognostic purposes.

Acknowledgements

This thesis came to fruition at a time when I had little contact with all those who've helped me and supported me. Nonetheless, there are so many people that I'd like to thank for helping me achieve this milestone in my life, all of whom I wish I could mention by name.

I'd like to start with thanking my dear friend and colleague Adianes, who has been with me from the time I joined the LMB Lab at the ARiEAL Research Center. Thank you for supporting and mentoring through my transition into clinical research. From our testing sessions over the pandemic, to our virtual calls – your support has helped me push myself to learn and grow as an academic.

To Chia-Yu - thank you for keeping me connected with my peers and faculty through this time. Your organization, coordination and ability to push the grain not only as a manager, but through the process of exploring your passions with the students are unparalleled; always inspiring me to learn more about my skillsets and integrate them with my passions. Thank you for always being available for a quick chat and keeping ARiEAL thriving.

To the LMB and ARiEAL members and service staff – thank you for your help in keeping the lab running and giving me a safe and productive space to complete my thesis.

To my family and dear friends Alice, Aditya and Teagan – you helped me stay on track and remember my love for my work, no matter how difficult the times were. Thank you for helping me challenge myself, but also showing me how to learn to enjoy that process.

Last but not certainly least, I am so grateful to my supervisory committee – Dr. John Connolly, Dr. James Reilly and Dr. Ian Bruce for making the process of completing a master’s thesis manageable through the pandemic. Thank you for showing me how to hone my skills and push myself to think out of the box. A big thank you to John for always humoring our conversations, but also keeping me on track. Thank you for introducing me to this amazing field of research and helping me find my love for clinical patient-centered research. Being a part of your team has been an uplifting and life-changing experience.

Table of contents

Lay abstract	iii
Abstract	iv
Acknowledgements	vi
Table of Contents	viii
List of Figures and Tables	x
List of All Abbreviations and Symbols	xii
1. Introduction	1
1.1. Neurophysiological methods, EEG-ERP.....	2
1.2. Disorders of Consciousness	3
1.3. Utility of EEG-ERPs in a Clinical Setting	4
1.4. The N400	4
1.5. N400 in clinical settings	5
1.6. Issues with previous N400 paradigms	6
1.7. N400s in response to non-visual and non-linguistic stimuli	7
1.8. This study	8
2. Methods	9
2.1. Participant	9
2.2. Stimuli	9
2.3. Electroencephalography Software and Equipment Settings...	10
2.4. EEG-ERP group level & single level statistical analysis	13
2.4.1. Group level	14
2.4.2. Single level	14
3. Results	16
3.1. Group level analyses	16
3.1.1. N100 Component	16
3.1.2. P200 Component	17
3.1.3. P3b Component	17
3.1.4. N400 Component	18
3.2. Single Subject Level Analyses	25
3.2.1. Pilot01	25
3.2.2. Pilot09	27
3.2.3. Pilot10	29
3.2.4. Ctrl04	31
3.2.5. Ctrl09	33

3.2.6.	Ctrl11	35
3.3	UWS Patient	37
4.	Discussion	40
4.1.	N100 and P200 components	42
4.2.	P3b component	42
4.3.	N400 Component	45
4.3.1.	Group level analysis	45
4.3.2.	Single subject analysis	46
4.4	UWS Patient analysis	47
4.4.	Limitations & future directions	47
5.	Conclusion	49
6.	References	50
7.	Appendices	58
7.1.	Appendix A	58

List of Figures and Tables

Figure 1: *Sequence of prime sounds and target words comprised in each trial, with the interstimulus interval (ISI) and intertrial interval (ITI).*

Figure 2: *Scalp distribution of the grand average of the N100 activity from 18 healthy participants.*

Figure 3: *Scalp distribution of the grand average of the P200 activity from 18 healthy participants.*

Figure 4: *Scalp distribution of the grand average of N400 activity for 18 healthy participants.*

Figure 5: *Graphs of the grand average ERPs in 18 healthy participants over a frontal (Fz), a central (Cz), and a parietal (Pz) electrode.*

Table 1: *F-statistics and p-values for the main effect of amplitude of condition, electrode, and interaction between condition and electrode for the N400 component 28*

Figure 6: *Scalp distribution of N400 activity over 350-600ms for healthy participant “pilot01”.*

Figure 7: *Scalp distribution of N400 activity over 350-600ms for healthy participant “pilot09”.*

Figure 8: Scalp distribution of N400 activity over 350-600ms for healthy participant “pilot10”.

Figure 9: Scalp distribution of N400 activity over 350-600ms for healthy participant “ctrl04”.

Figure 10: Scalp distribution of N400 activity over 350-600ms for healthy participant “ctrl09”.

Figure 11: Scalp distribution of N400 activity over 350-600ms for healthy participant “ctrl11”

Figure 12: Scalp distribution of N400 activity over 350-600ms for a UWS patient 40

Figure 13: Graph depicting congruent (black) and incongruent (blue) waveforms over 3 frontal, 3 central and 3 parietal electrodes for a UWS patient.

Figure 14: Graphs depicting congruent (black) and incongruent (blue) waveforms over 3 frontal, 3 central and 3 parietal electrodes of the grand average of 18 healthy participants.

Figure 15: Graphs depicting differences between the t-values for the congruent and incongruent condition reliably detected by permutations t-test ($p < 0.05$) of the grand average of 18 healthy participants. Significant intervals are denoted by the gray areas.

Figure 16: *Graphs of the ERPs in 'pilot01' over the P4, mean of the 3 parietal (P3, Pz, P4) and mean of the 6 centro-parietal (C3, P3, Cz, Pz, C4, P4) electrodes.*

Figure 17: *Graphs of the ERPs in 'pilot09' over the Fz, F4, mean of the 3 frontal (F3, Fz, F4), C4, and mean of the 6 fronto-central (F3, C3, Fz, Cz, F4, C4) electrodes.*

Figure 18: *Graphs of the ERPs in 'pilot10' over the Fz electrode. A) Grand averaged waveforms for the congruent condition represented by the black waveform, and the incongruent condition, represented by the blue waveform.*

Figure 19: *Graphs of the ERPs in 'ctrl04' over the C3, mean of the 3 central (C3, Cz, C4), mean of the 6 fronto-central (F3, C3, Fz, Cz, F4, C4) and mean of the 6 centro-parietal (C3, P3, Cz, Pz, C4, P4) electrodes.*

Figure 20: *Graphs of the ERPs in 'ctrl09' over the Pz electrode. A) Grand averaged waveforms for the congruent condition represented by the black waveform, and the incongruent condition, represented by the blue waveform.*

Figure 21: *Graphs of the ERPs in 'ctrl11' over the C3, Cz, mean of 3 central (C3, Cz, C4) and mean of the 6 fronto-central (F3, C3, Fz, Cz, F4, C4) electrodes.*

List of Abbreviations and Symbols

ANOVA: Analysis of Variance

BVA: BrainVisionAnalyzer

dB: Decibels

df: Degrees of Freedom

DOC: Disorders of Consciousness

EEG: Electroencephalography

ERP: Event-Related Potentials

Hz: Hertz

ICA: Independent Component Analysis

ISI: Inter-Stimulus Interval

ITI: Inter-Trial Interval

MCS: Minimally Conscious State

ms: Milliseconds

SD: Standard Deviation

UWS: Unresponsive Wakefulness State

VS: Vegetative State

μV : Microvolts

1. Introduction

The aim of this thesis was to gain more insight into the effects of traumatic brain injury and stroke, and neurodegenerative conditions such as Alzheimer's disease, Parkinson's disease, Amyotrophic Lateral Sclerosis and other conditions that are associated with altered states of consciousness. This thesis addresses the issues that arise from reliance on behavioral scales dependent on overt observable signs of cognitive and sensory function. The utilization of behavioral scales in clinical settings is associated with unreliable diagnoses, calling for the need for brain imaging for accurate assessment of patients (Giacino et al., 2010; Seel et al., 2010).

The reliance on behavioral scales for differentiating between UWS and Minimally Conscious State (MCS) has resulted in high rates of misdiagnoses in these patients, due to their fluctuating periods of wakefulness and attentiveness (Schnakers et al., 2009, Wannez et al., 2017). A study by Schnakers and colleagues in 2009 reported up to 41% of patients who were misdiagnosed with UWS were found to be in MCS. Connolly et al. (1999) were the first to study cognitive function in non-communicative patients in UWS. Following this work, several other findings have also explored brain function in coma patients (Laureys et al., 2014), to estimate outcomes (Armanfard et al., 2019; Fischer et al., 1999; Holekova et al., 2008; Fischer, Dailler, & Morlet, 2008; Morlet and Fischer, 2014).

The neuroimaging method chosen to assess brain function is based on the objective of the assessment. The overall objective of this work was to assess a wide range of low-level to higher order cognitive functions such as memory, attention, and language

comprehension and production. Considering this objective, the imaging method chosen should be able to evaluate the speed of the responses as an estimate of the quality of brain function (i.e., the latency), and the strength of the response as a measure of the quality of brain function, depicted by the amplitude. Finally, the imaging technique should also ideally be accessible as a bedside point of care system (Duncan et al, 2009).

1.1 Neurophysiological methods, EEG-ERP

Several electrophysiological methods such as electroencephalography (EEG), and functional imaging methods such as fMRI (functional magnetic resonance imaging) and PET (positron emission tomography) have provided more quantitative and sensitive assessments of sensory and cognitive activity in these non-communicative patients (Giacino et al., 2014).

EEG, and specifically event-related potentials (ERPs), which are time-locked electrical brain activity extracted from continuous EEG recordings in response to specific stimuli, have been observed to be useful in assessing a wide range of early sensory to later complex and higher order cognitive functions such as memory, attention, and language comprehension and production (Kutas & Ferdermier, 2011; Duncan et al., 2009).

EEG-ERPs provide a non-invasive, and portable avenue to record and analyze a wide range of brain activity, which makes it a great tool for research and clinical purposes. Additionally, its excellent temporal resolution allows it to monitor and record

minor fluctuations in cognitive activity and other clinical functions (Gawryluk et al., 2010; Duncan et al., 2009; Gosseries et al., 2014).

1.2 Disorders of Consciousness

Patients with severe acquired brain injuries are sometimes affected by a set of conditions called Disorders of Consciousness (DOC), characterized by altered states of consciousness. DOCs are generally identified and defined by their behavioral features with reference to their level of consciousness (Giacino et al., 2014). Coma is defined by a state of unresponsiveness where the patient's eyes are closed and cannot respond to any stimulation, which can result from traumatic brain injury, cardiac arrest, stroke, brain tumor, metabolic infectious disease or drug intoxication. A coma can last for a few weeks after which patients can recover or emerge into one of two states: Unresponsive Wakefulness Syndrome (UWS), also called Vegetative State (VS), or Minimally Conscious State (MCS). Patients in UWS tend to show spontaneous eye-opening, but no awareness of the environment or themselves. Patients in MCS on the other hand show inconsistent and minimal intentional behaviors indicating environmental or self-awareness, in some cases indicating a good prognosis (Giacino et al., 2014).

1.3 Utility of EEG-ERPs in a clinical setting

Clinical neuroimaging research efforts using EEG-ERPs have been observed to be reliable for the assessment of effects of traumatic brain injuries, seizures and other neurological conditions (Duncan et al, 2009), and for predicting the prognoses of these

patients have been widely reported over recent years. (Duncan et al, 2009). Several other studies have also reported findings showing induced sensory and cognitive activity in coma patients, which could be used to suitably diagnose, and accurately estimate their prognoses. Specifically, these studies reported earlier ERPs indicating the functioning of auditory sensory pathways preceding higher cognitive functions associated with memory, attention, concentration and speed of mental processing (Fischer et al., 1999; Duncan et al, 2009; Morlet& Fischer, 2014; Holekova et al., 2008; Fischer, Dailler, & Morlet, 2008; Naccache et al., 2005). This thesis will explore the use of the ERP called the N400 linked to these higher cognitive processes.

1.4 The N400

The N400 is a negative-going waveform that peaks at around 400 ms that is observed in response to meaningful stimuli such as words, pictures, music and environmental sounds. (Kutas & Ferdermeier, 2011). The N400 was discovered by Marta Kutas and Steven Hillyard in the 1980s, when evaluating the responses to a paradigm that used sentences ending with semantically congruent or incongruent words. For instance, the sentence “The cat climbed on the ___” showed more N400 activity in response to an unexpected word like “bread”, as opposed to the word “tree”. They observed higher amplitude N400 activity in response to words that were semantically unrelated to the context of the sentence, compared to the N400 amplitude in response to the sentences that ended with congruent words. The difference between the amplitudes observed in response to the incongruent and congruent conditions is referred to as the N400 effect, which reflects the overall processing and comprehension

of meaningfulness (Kutas and Hillyard, 1980). This N400 effect has also been observed in response to unrelated target words in word pairs. For instance, a related word pair “table-chair” would show a smaller N400 component compared to an unrelated word pair like “table-cloud”. These words were unrelated to the priming word either identically, associatively, semantically, categorically, and possibly phonologically (D’Arcy et al., 2004; Kutas and Ferdermeier, 2011). The N400 component has been observed in response to words presented visually and/or auditorily in sentences and word-pairs paradigms alike in subsequent studies (Kutas & Ferdermeier, 2011; Connolly et al., 1995; Holcomb and Anderson 1993).

1.5 N400 in clinical settings

Upon the establishment of the N400 component as a reliable ERP measure to understand language comprehension and conceptual processing, the potential of its utility to assess cognitive function in various clinical populations was explored (Morlet et al., 2013; Connolly et al., 1995). While there is a growing literary database of findings reporting the application of various ERPs for diagnostic and prognostic purposes (Kutas & Ferdermeier 2011; Kotchoubey et al, 2005; Rämä et al., 2010), there are minimal findings exploring the ability of N400 to assess the processing of meaningful stimuli in coma patients. The existing findings have been observed mainly in response to semantic priming experiments, which involved meaningful target stimuli succeeding semantically related or unrelated prime meaningful stimuli (Kotchoubey et al, 2005; Rämä et al., 2010; Daltrozzo et al. 2009; Balconi & Arangio, 2015). For instance, Kotchoubey and colleagues were the first to report the N400 effect indicating linguistic

processing in response to a sentence priming and a word-pair priming paradigm in a coma patient. Following this pioneering study, several other studies also reported observing the N400 effect in coma patients in response to sentence priming and word pair priming paradigms (Daltrozzo et al. 2009; Balconi & Arangio, 2015; Rämä et al., 2010).

1.6 Issues with previous N400 paradigms

A majority of the previously mentioned reputed studies reported findings mainly in response to the word pair and sentence priming experiments (Kutas and Ferdermier, 2011). These priming paradigms using linguistic stimuli can only be tested on fluent and native speakers of the language to obtain reliable results. Additionally, most of these findings were seen in response to stimuli administered only visually, or a combination of the visual and auditory modalities (Kutas and Ferdermeier, 2011; Cummings et al., 2006; Orgs et al., 2006). Such paradigms cannot be administered to patients with altered and fluctuating states of consciousness. Finally, the exclusive use of linguistic stimuli, often in complex forms such as sentences may make it difficult for non-responsive patients to respond properly as these stimuli may tax the working memory (D'Arcy et al, 2005).

1.7 N400s in response to non-visual and non-linguistic stimuli

Currently, there is a dearth in studies reporting findings that used non-linguistic auditory stimuli in priming paradigms, such as music and environmental sounds

(Koelsch et al. 2004; Van Petten and Rheinfelder, 1995; Cummings et al., 2006).

Environmental sounds, defined as sounds related to real events (e.g., cat meowing, or footsteps) with contextual cues which have meaning similarly to words could address this gap. These sounds are primed in our memory with reference to specific events and concepts, dependent on familiarity and frequency of occurrence (Ballas & Howard, 1987; Cummings et al., 2006). Van Petten and Rheinfelder were the first to use exclusively auditory stimuli in the form of non-linguistic (i.e., environmental sounds) and linguistic (i.e., words) in a priming paradigm in 1995 to investigate processing of meaningful stimuli in native English speakers. This study showed that the N400 component seen in response to the auditory sound-word pairs were indistinguishable from the N400 elicited by a word–word pair (Van Petten & Rheinfelder, 1995).

Subsequent studies that have used environmental sounds in priming paradigms emulating Van Petten and Rheinfelder’s work have mostly been conducted with visual or both visual and auditory stimuli to assess language processing (Van Petten & Rheinfelder, 1995; Orgs et al., 2006; Cummings et al., 2006). However, there are no studies that have tested N400 priming paradigms to assess cognitive activity in response to auditory non-linguistic conceptually meaningful stimuli in coma patients.

1.8 This study

This thesis aims to bridge this gap in the existing literature by examining whether a unimodal auditory priming paradigm consisting of the pairing of non-linguistic stimuli in the form of environmental sounds and linguistic stimuli in the form of spoken words can

induce the N400 effect. In conjunction with previous literature on conceptual and semantic priming experiments of different modalities (Van Petten et al., 1995; Cummings et al., 2006; Orgs et al., 2006), we hypothesize that the N400 effect will be observed in response to conceptually incongruent environmental sounds paired with spoken words (Van Petten et al., 1995; Cummings et al., 2006; Orgs et al., 2006). The ultimate goal of this study is for the implementation of such a priming paradigm for diagnostic and prognostic purposes for various patient populations with neurological dysfunction, such as coma patients, who are unable to easily comprehend and respond appropriately to complex linguistic stimuli. This paradigm was tested on healthy native English-speaking individuals to investigate if it could induce the N400 effect across the group in a manner similar to Van Petten and Rheinfelder's findings.

In order to develop a paradigm for diagnostic and prognostic potential, it is essential to evaluate the single subject sensitivity of the N400 effect in response to this auditory sound-word priming paradigm. Thus, we also hypothesize that the N400 effect will be observed on a single subject level. The implication of this work could pave the way for the development of electrophysiological and machine learning procedures using EEG-ERPs for emergence from coma and prediction of prognoses for such patients.

2. Methods

2.1 Participants:

This study included 18 native English-speaking participants (3 males, 15 females), aged between 18-45 years (mean=20.27). Two of the male participants, and one female had

a history of concussions, and one participant had received the diagnosis of dyslexia. Participants were paid \$15/hour, to a maximum of \$180 and the study was approved by the Hamilton Integrated Research and Ethics Board (HiREB).

2.2 Stimuli:

The stimuli consisted of environmental sounds and spoken words. The sounds were used as primes, and they were paired with either conceptually related or conceptually unrelated spoken words, which were the targets.

Environmental sounds: Environmental sounds chosen were based on the following four categories – animal sounds (e.g., cat meowing), non-human speech sounds (e.g., coughing), alarms/alerts (e.g., police siren), and everyday sounds (e.g., footsteps), adapted from previous similar paradigms (Van Petten & Rieffers, 1995; Orgs et al., 2006). A total of 122 sounds were selected, and modified to a uniform duration of 1500ms, and their intensity was normalized to 80 dB on 'PRAAT', a software for speech analysis, and 70 dB on 'Audacity', an audio recorder and editor software.

Spoken-words: Additionally, 122 spoken words were created using 'ReadSpeaker', a text-to-speech software, simulating a female native speaker of American English in a neutral tone of voice to be paired with the sounds. The spoken words were also normalized to 80 dB using 'PRAAT.' The spoken words were selected based on a pilot experiment that used a Likert scale of 0 - 10, with 0 referring to no conceptual associations, and 10 referring to a high level of conceptual relatedness between the primes and targets. For instance, the sound of a dog barking would be very closely

related conceptually to the spoken word 'dog', but weakly conceptually related to a word like 'shirt'.

A subsequent pilot experiment was conducted to assess the comprehensibility of the sounds. A total of 19 native English-speaking participants were asked to listen to a series of 122 sounds and label them. Trials were selected for removal based on whether the participants were able to identify the sounds accurately up to 50% of the time. The trials were then manually filtered out from the raw data, preprocessed on BrainVisionAnalyzer 2.012.01, as explained below. Upon preliminary manual correction and subsequent preprocessing, there were no visible improvements in the data. Thus, this reanalysis process was not completed.

2.3 Electroencephalography Software and Equipment Settings:

The auditory stimuli were presented to the participants using earphones (Etymotic ER-1) and Presentation software (Neurobehavioral Systems). The environmental sounds (primes) were separated from the spoken words (targets) by an interstimulus interval (ISI) of 2100ms, and every trial comprised of the prime and target were separated from each other by an interval (ITI) of 3200ms (Van Petten & Rheinfelder, 1995) as can be seen in Figure 1.

EEG data was collected using a 64 channel Biosemi ActiveTwo system (Biosemi, Amsterdam, The Netherlands), filtered with a bandpass filter of 0.01–100 Hz and digitally sampled at 512 Hz. The electrodes were placed on the scalp according to the modified 10/20 positioning using a 64-electrode cap. Vertical and horizontal

electrooculogram signals were monitored by electrodes placed above and over the outer canthus of the left eye. References were recorded at the nose and from bilateral mastoids for offline referencing.

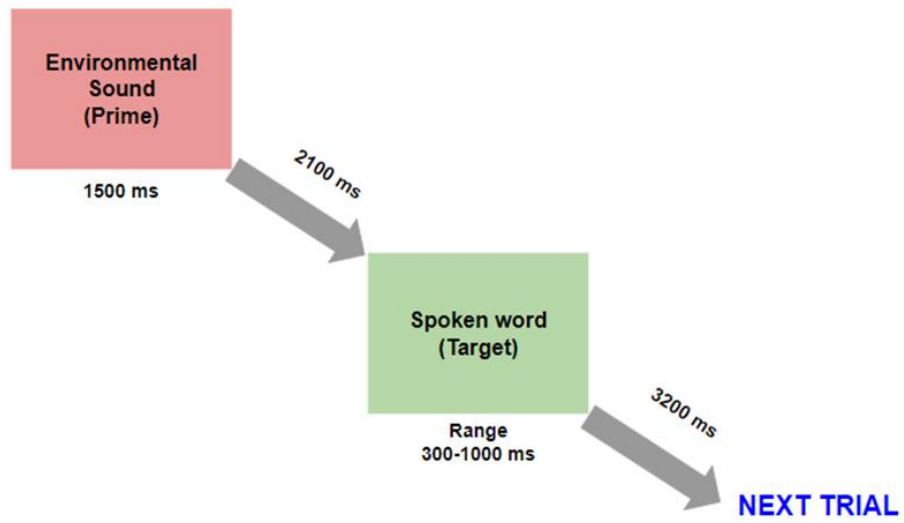


Figure 1: Sequence of prime sounds and target words comprised in each trial, with the interstimulus interval (ISI) and intertrial interval (ITI).

2.4 EEG-ERP group level & single level statistical analysis

Preprocessing was performed using BrainVisionAnalyzer 2.012.01 (BrainProducts). The data was digitally filtered offline using the IIR Butterworth filters with a bandpass of 0.1 to 30 Hz. IIR filters are usually used when there is no defined phase information, such as for signal amplitudes, while FIR filters (Cheveigne & Nelsen, 2019) are used for linear phase responses. A Butterworth filter is a type of signal processing filter used to have a flat frequency bandpass (Cheveigne & Nelsen, 2019). An Independent Component Analysis (ICA) was performed to correct ocular vertical and horizontal artifacts. Recordings were visually inspected and segments containing artifacts (e.g., muscle activity, movements) were removed. For each individual, the data was segmented and base-line-corrected into epochs of -100 ms before and 700 ms after stimulus presentation and averaged for congruent and incongruent conditions. Semi-automated peak detection was conducted to determine the most negative points between 400-600 ms for the N400 component. Amplitude and latency values were averaged 25 ms before to 25 ms after the identified peaks and subsequently exported to be statistically analyzed. Grand averages were created based on the data from all 18 participants for each condition to visually determine the presence of these components.

Permutation t-test: Permutation tests are non-parametric statistical methods that are not compromised by some of the issues of parametric statistics such as the requirement of known distributions. Unlike traditional significance tests, which rely on normal distributions, permutation testing relies on resampling to create a sampling distribution. It also relies less on the parameters that common significance tests use, such as adhering to normal distributions for t-tests and ANOVAs, for example. Permutation tests

are more sensitive and are better than parametric tests for smaller sample sizes since they rely on random sampling, compared to traditional tests where reduction in sample size affects statistical power.

2.4.1 Group level:

1. Permutation t-test: One tailed serial permutation t-tests were performed over a mean of 9 front, central and parietal electrodes to identify where the N400 effect, i.e., higher negative amplitude of N400 in response to incongruent sound-word pairs compared to N400 amplitude peaks in response to congruent sound-word pairs could be seen. For group-level analyses, dependent samples permutation-t testing was performed across individual-averaged ERPs for the entire epoch (-100 to 700 ms).
2. Mixed effects Analysis of variance (ANOVA): This analysis was performed using R statistical software v3.3.3 and the ez12 package v4.4-0 and two within-subject factors were considered – condition and electrodes. The condition factor has two levels – congruent and incongruent, and the electrodes have 9 levels – 3 frontal, 3 central and 3 parietal electrodes. Mauchly's sphericity test was used to determine sphericity, and Greenhouse-Geisser estimates were computed to correct degrees of freedom to reduce chances of type 1 error (Orgs et al., 2006).

2.4.2 Single level:

Permutation t-test: For single-subject analyses, independent samples permutation t-tests were conducted across trials from each subject. For both analyses, the number of

permutations was set to 1000, the p-values were corrected using the tmax statistic for multiple comparisons.

This thesis aimed to look at whether significant N400 activity could be seen over the traditional grand averages, but also over individual participants. Assessing the reliable occurrence of this activity across individuals is essential to examine if such a protocol is sensitive enough to induce cognitive activity in individuals with neurological dysfunction, such as patients with DOCs.

3. Results

The N400 waveforms, along with two other waveforms that were also observed, the N100 and P200, were analyzed over 3 frontal (F3, Fz, F4), 3 central (C3, Cz, C4) and 3 parietal (P3, Pz, P4) electrodes across the grand average of 18 participants. Graphs of the difference between the t-statistic values for the congruent and incongruent condition for the grand average for these electrodes and means of groups of frontal, central, parietal, fronto-central, fronto-parietal, centro-parietal, were created to show the significance between the conditions for the N400 component, detected by permutations t-test ($p < 0.05$). Additionally, these graphs of the difference between the t-values for the congruent and incongruent condition for these electrodes were also created for 6 out of the total 18 healthy participants who showed significant differences between the congruent and incongruent conditions ($p < 0.05$). Statistical differences between the congruent and incongruent conditions were examined to see if such a protocol can be seen in individuals, alongside across the grand averages to see if such a protocol can be sensitive enough to induce the N400 components in patients with DOCs.

3.1 Group level analyses

3.1.1 N100 Component

The N100 was defined as a negative peak that was observed typically between 100 ms and 200 ms. The N100 peak amplitude of the congruent waveform ($M = -1.475 \mu V$, $SD = 1.039 \mu V$) was observed to be larger than the incongruent waveform ($M = -0.622$

μV , $\text{SD}=0.866 \mu\text{V}$), which can be seen from the scalp distribution this ERP component in Figure 2. Additionally, the N100 peak of the congruent waveform ($M=145 \text{ ms}$, $\text{SD}=24.8 \text{ ms}$) was observed to reach maximum amplitude at approximately the same time as the incongruent N100 peak ($M=149 \text{ ms}$, $\text{SD}=27 \text{ ms}$).

The mixed-model design ANOVA showed significant main effects for the amplitude for the condition [$F(1,17)=17.699$, $p<0.001$], electrode [$F(8,136)=5.242$, $p=0.004$] and for condition x electrode [$F(8,136)=3.680$, $p=0.045$] interactions. However, the mixed-model design ANOVA did not show significant differences for the condition, electrode nor for condition x electrode interactions when analyzing latency of this component.

Serial permutation t-tests for the condition showed no significant differences in latency for the congruent and incongruent condition over any of the 9 electrodes for this component.

3.1.2 P200 Component

A positive peak was observed after the N100 and just before the N400 component between 200 ms and 300 ms, the P200. The amplitude of the incongruent P200 peak was observed to be higher in amplitude ($M=1.79 \mu\text{V}$, $\text{SD}=1.32 \mu\text{V}$) compared to the P200 peak for the congruent condition ($M=1.26 \mu\text{V}$, $\text{SD}=1.2 \mu\text{V}$) (Figure 3). The P200 peak of the congruent waveform ($M=259 \text{ ms}$, $\text{SD}=31.1 \text{ ms}$) was observed to reach maximum amplitude at approximately the same time as the incongruent N400 peak ($M=248 \text{ ms}$, $\text{SD}=28 \text{ ms}$).

The mixed-model design ANOVA confirmed a significant main effect of condition [$F(1,17)=7.000$, $p=0.017$] and a significant main effect of electrode_x_condition interaction for latency [$F(8,136)=4.031$, $p=0.005$]. A significant main effect of amplitude effect of condition [$F(1,17)=9.633$, $p=0.006$] and a significant main effect of electrode [$F(8,136)=19.126$, $p<0.001$] were also observed for this component.

Serial permutation t-tests for the condition showed significant differences in the t-value for the congruent and incongruent condition slightly earlier over the Fz and C3 electrodes between 100 and 200ms, and between 200 and 300 ms over the Cz electrode (see Figure 15 in Appendix A).

3.1.3 P3b Component

Another slight positive-going peak can be seen upon visual inspection on the congruent waveform over two of the frontal (Fz, F4), two central (Cz, C4) and two parietal (Pz, P4) electrode, and over the C3 and P3 electrode on the incongruent waveform between 300 and 400ms (Figures 5a, 14).

3.1.4 N400 Component

The N400 effect provides information on the processing of meaningful stimuli through a priming experiment. The topographical maps exhibit mainly centro-parietal distribution of the N400 component over the scalp. The amplitude of the N400 peak observed for the incongruent condition ($M=-2.17\mu V$, $SD=1.67\mu V$) was slightly more

negative when compared to the amplitude of the peak for the congruent condition ($M=-1.18\mu\text{V}$, $SD=1.06\mu\text{V}$) as can be seen in Figure 4. The N400 activity showed lateral asymmetry; the peaks observed over the right hemisphere were larger than those over the left hemisphere, as can be seen in Figure 4. N400 peaks can be observed distributed over two frontal electrodes (Figure 14 in Appendix A). Additionally, the N400 peak of the incongruent waveform ($M=507\text{ ms}$, $SD=52.8\text{ ms}$) was observed to reach maximum amplitude at approximately the same time as the congruent N400 peak ($M=514\text{ ms}$, $SD=55.3\text{ ms}$). A mixed-model design ANOVA confirmed that there was a significant main effect of condition for amplitude of the N400 component [$F(1,17)=15.602$, $p<0.001$], a significant main effect of electrode [$F(8, 136)=25.751$, $p<0.001$] and condition \times electrode [$F(8,136)=5.347$, $p=0.001$] interaction (Table 1).

Serial permutation t-tests for the condition showed significant differences in the t-value for the congruent and incongruent condition over the Cz & Pz electrodes between 400 and 500 ms (see Figure 5). Additionally, significant differences in the t-value for the congruent and incongruent condition were also observed over the P3 electrode (see Figure 15 in Appendix A).

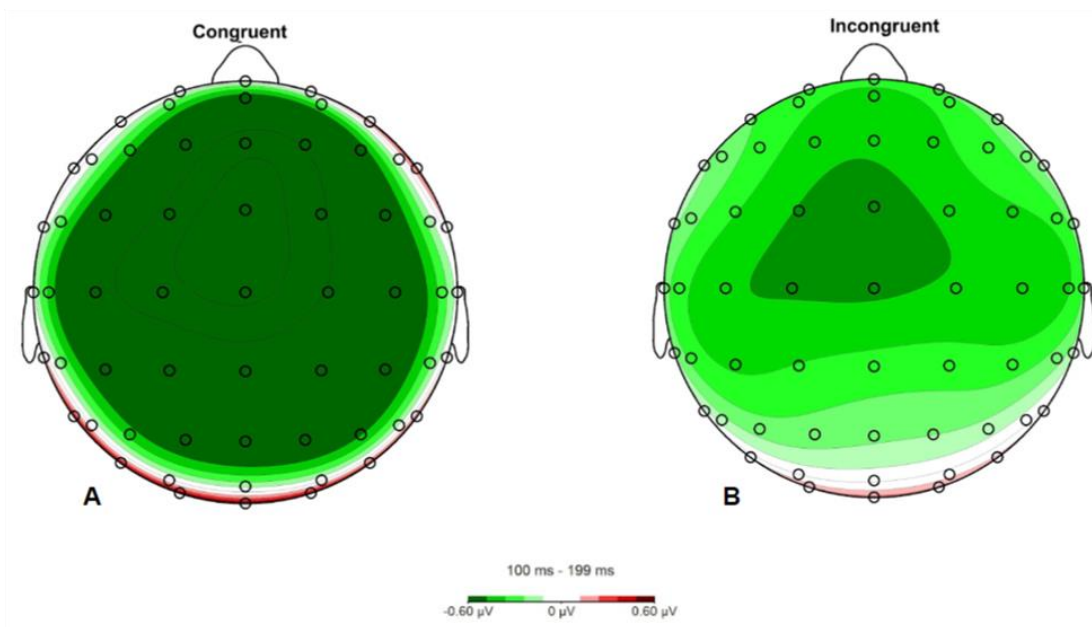


Figure 2: Scalp distribution of the grand average of the N100 activity from 18 healthy participants. The figure shows the topographical activities for the congruent (A) and incongruent (B) condition over the time interval of 100-200 ms. The color bar indicates the amplitudes of the peaks. Amplitude scales depicted are independent from amplitude scales for graphs with waveforms.

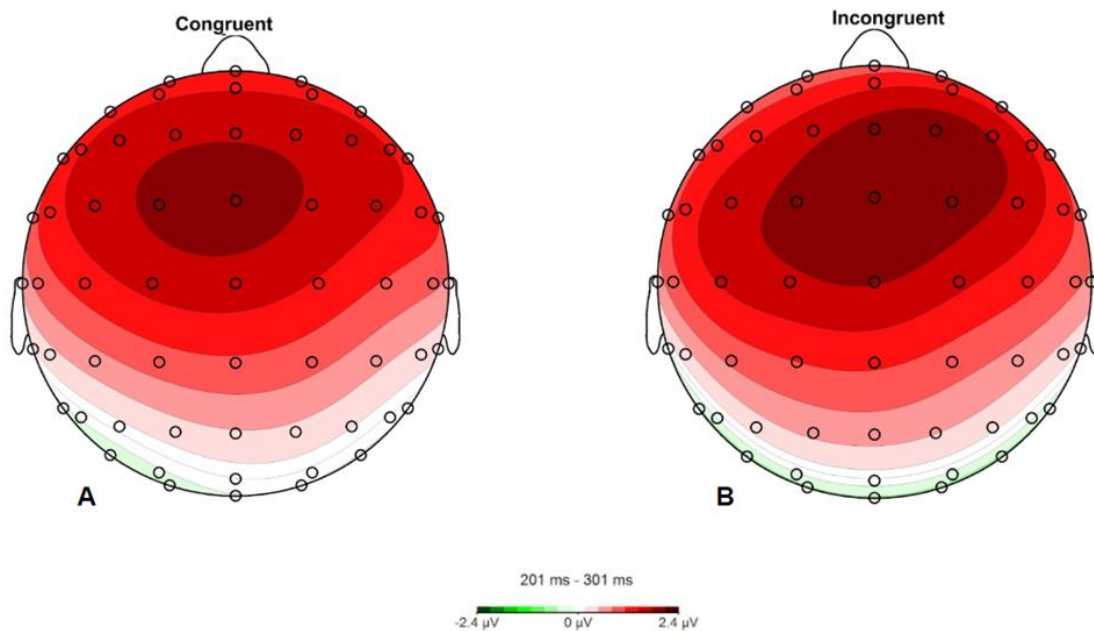


Figure 3: Scalp distribution of the grand average of the P200 activity from 18 healthy participants. The figure shows the topographical activities for the congruent (A) and incongruent (B) condition over the time interval of 200-300 ms. The color bar indicates the amplitudes of the peaks. Amplitude scales depicted are independent from amplitude scales for graphs with waveforms.

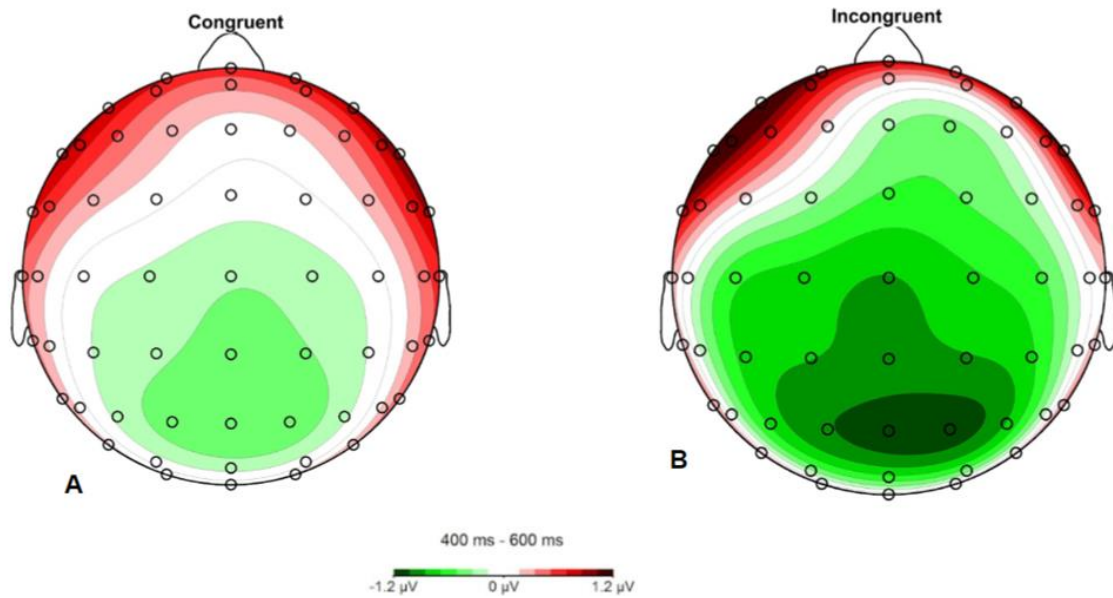


Figure 4: Scalp distribution of the grand average of N400 activity for 18 healthy participants. The figure shows the topographical activities for the congruent (A) and incongruent (B) condition over the time interval of 400-600 ms. The color bar indicates the amplitudes of the peaks. Amplitude scales depicted are independent from amplitude scales for graphs with waveforms.

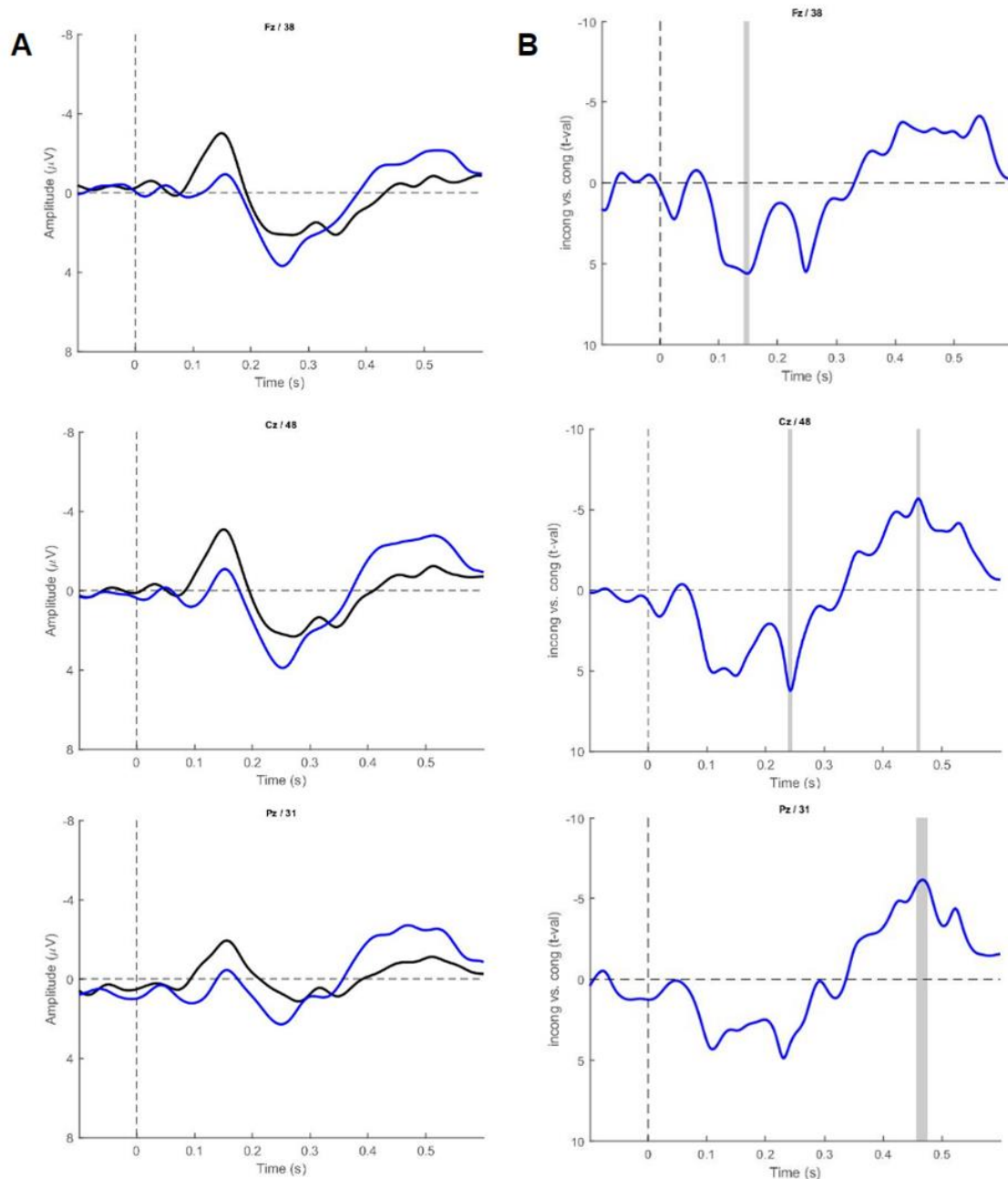


Figure 5: Graphs of the grand average ERPs in 18 healthy participants over a frontal (Fz), a central (Cz), and a parietal (Pz) electrode. A. Grand averaged waveforms for the congruent condition represented by the black waveform, and the incongruent condition, represented by the blue waveform. B. Difference between the t-values for the congruent and incongruent condition reliably detected by permutations t-test ($p < 0.05$). Significant intervals are denoted by the gray areas. The amplitude scales depicted are independent from amplitude scales for topographical maps.

Table 1: *F-statistics and p-values for the main effect of amplitude of condition, electrode, and interaction between condition and electrode for the N400 component. Significance ($p < 0.05$) indicated by *.*

Effect	F-statistic	p-value
Condition	15.602	1.0334e-03
Electrode	25.751	3.8906e-13
Cond:Elec	5.347	1.1115e-03

3.2 Single Subject Level Analyses

Out of the total 18 healthy participants tested, 6 of them showed significant differences in the N400 activity between congruent and incongruent conditions across the above mentioned 9 electrodes.

3.2.1 Pilot01

The topographical maps over the time interval of 300-400 ms shows more negative activity for the incongruent condition ($M=-2.38 \mu\text{V}$, $SD=0.67 \mu\text{V}$), compared to the response to the congruent condition ($M=-1.45 \mu\text{V}$, $SD=0.88 \mu\text{V}$) as can be seen in Figure 6b, over the central and parietal areas. The map for the congruent condition shows more negative activity over the parietal regions (Figure 6a). The peak of the incongruent waveform was observed earlier ($M=422\text{ms}$, $SD=50\text{ms}$) than the congruent waveform ($M=555$, $SD=41.8$).

The serial permutation t-test for the condition showed significant negative activity, as represented by the grey bars, between 300 and 400ms at the P4 electrode, the mean of the 3 parietal electrodes (P3, Pz, P4), the mean of the 6 central and parietal electrodes (C3, P3, Cz, Pz, C4, P4), and the mean of the 3 electrodes (P3, Pz, P4) (see Figure 16 in Appendix A).

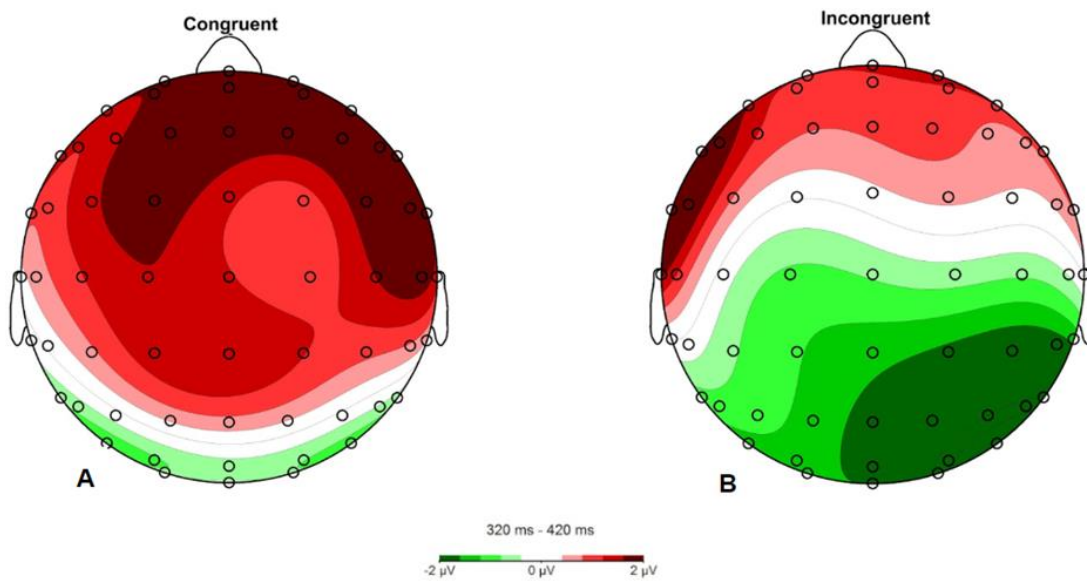


Figure 6: Scalp distribution of N400 activity for healthy participant “pilot01”. The figure shows the topographical activities for the congruent (A) and incongruent (B) condition over the time interval of 320-420 ms. The color bar indicates the amplitudes of the peaks. Amplitude scales depicted are independent from amplitude scales for graphs with waveforms.

3.2.2 Pilot09

The topographical maps over the time interval of 300-400 ms show more negative activity mainly over the frontal, central, and parietal regions for the incongruent condition ($M=-3.14 \mu\text{V}$, $SD=0.74 \mu\text{V}$), as indicated in Figure 7b, compared to the congruent condition ($M=-1.06 \mu\text{V}$, $SD=0.35 \mu\text{V}$) (Figure 7a). The peak of the incongruent waveform was observed earlier ($M=485\text{ms}$, $SD=27.5\text{ms}$) than the congruent waveform ($M=488$, $SD=41.8\text{ms}$).

The serial permutation t-test for the condition indicated a significant difference between the congruent and incongruent conditions as represented by the gray bars, between 300 and 400ms at the F4, Fz and C4 electrodes, and the mean of 6 frontal and central electrodes (F3, C3, Fz, Cz, F4, C4) (see Figure 17 in Appendix A).

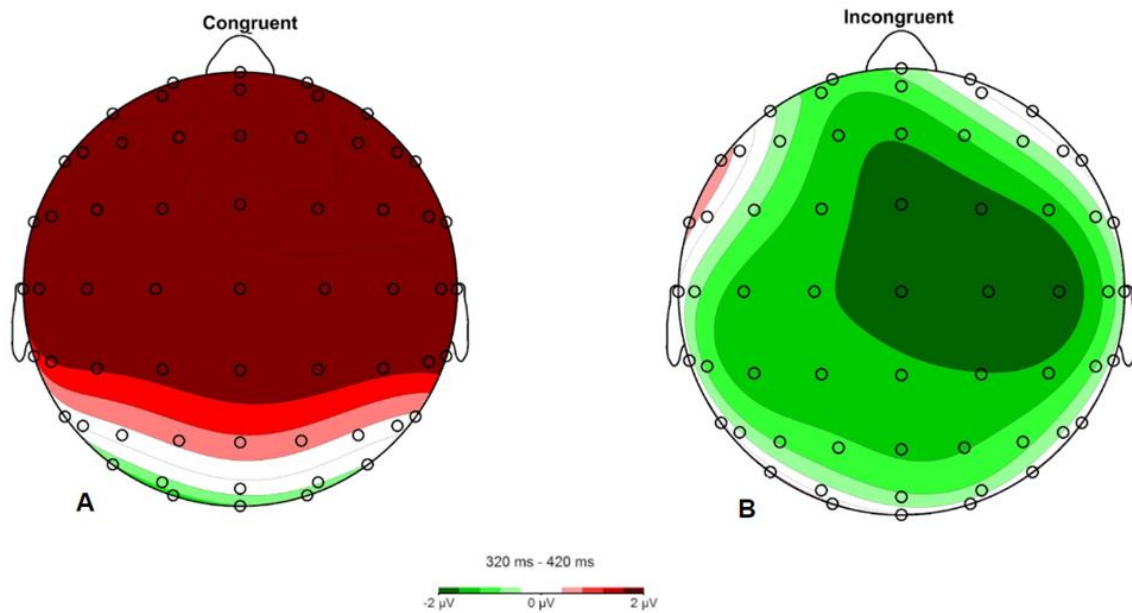


Figure 7: Scalp distribution of N400 activity for healthy participant “pilot09”. The figure shows the topographical activities for the congruent (A) and incongruent (B) condition over the time interval of 320-420 ms. The color bar indicates the amplitudes of the peaks. Amplitude scales depicted are independent from amplitude scales for graphs with waveforms.

3.2.3 Pilot10

The topographical map for the incongruent shows more negative activity ($M=-2.17 \mu\text{V}$, $SD=1.63 \mu\text{V}$) mainly over the central and parietal areas, and frontal region, distributed over the right hemisphere (Figure 8b). The map for the congruent condition shows less negative activity compared to the incongruent condition ($M=-1.66 \mu\text{V}$, $SD=0.69 \mu\text{V}$) over the central area and parietal regions, as indicated in Figure 8a. The peak of the incongruent waveform was observed earlier ($M=502\text{ms}$, $SD=29.7\text{ms}$) than the congruent waveform ($M=563$, $SD=41.2\text{ms}$).

The serial permutation t-test for the condition indicated a significant difference between the congruent and incongruent conditions as represented by the gray bars, between 500 and 600ms at the Fz electrode (See Figure 18 in Appendix A).

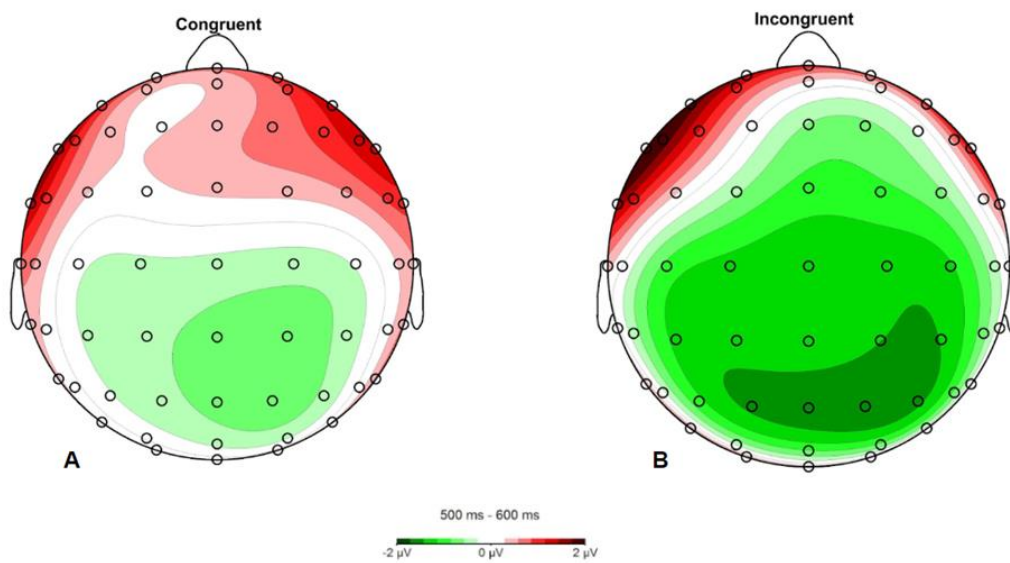


Figure 8: Scalp distribution of N400 activity for healthy participant “pilot10”. The figure shows the topographical activities for the congruent (A) and incongruent (B) condition over the time interval of 500-600 ms. The color bar indicates the amplitudes of the peaks. Amplitude scales depicted are independent from amplitude scales for graphs with waveforms.

3.2.4 *Ctrl04*

The topographical map of the incongruent condition shows more negative activity ($M=-2.21\mu V$, $SD=1.39\mu V$) mainly over the central and parietal areas, as can be seen Figure 9b. Comparatively, the map for the congruent condition shows less negative activity ($M=-0.62\mu V$, $SD=0.40\mu V$) over the central area (Figure 9a). The peak of the congruent waveform was observed earlier ($M=496$, $SD=48.7ms$) than the incongruent waveform ($M=543ms$, $SD=17.9ms$)

The serial permutation t-test for the condition indicated a significant difference between the congruent and incongruent conditions as represented by the gray bars at the C3 electrode, and the mean of 3 central electrodes (C3, Cz, C4), mean of 6 frontal and central electrodes (F3, C3, Fz, Cz, F4, C4) and the mean of the central and parietal electrodes (C3,P3, Cz, Pz, C4, P4) (See Figure 19 in Appendix A).

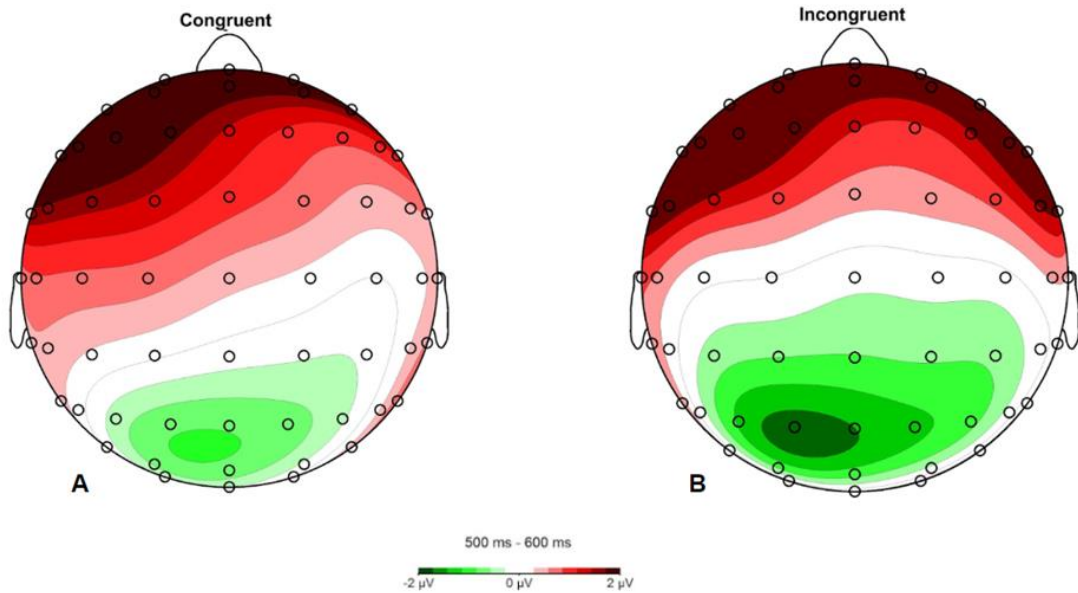


Figure 9: Scalp distribution of N400 activity for healthy participant “ctrl04”. The figure shows the topographical activities for the congruent (A) and incongruent (B) condition over the time interval of 500-600 ms. The color bar indicates the amplitudes of the peaks. Amplitude scales depicted are independent from amplitude scales for graphs with waveforms.

3.2.5 *Ctrl09*

The topographical map of the incongruent condition mainly shows more negative activity ($M=-0.44 \mu\text{V}$, $SD=0.86 \mu\text{V}$) mainly over the parietal areas, as can be seen Figure 10b, compared to the map of the congruent condition ($M=0.13 \mu\text{V}$, $SD=0.60 \mu\text{V}$) (Figure 10a). The peak of the congruent waveform was observed earlier ($M=538$, $SD=34.4\text{ms}$) than the incongruent waveform ($M=548\text{ms}$, $SD=58.5\text{ms}$)

The serial permutation t-test for the condition indicated a significant difference between the congruent and incongruent conditions, as represented by the gray bar, between 400 and 500ms at the Pz electrode (see Figure 20 in Appendix A).

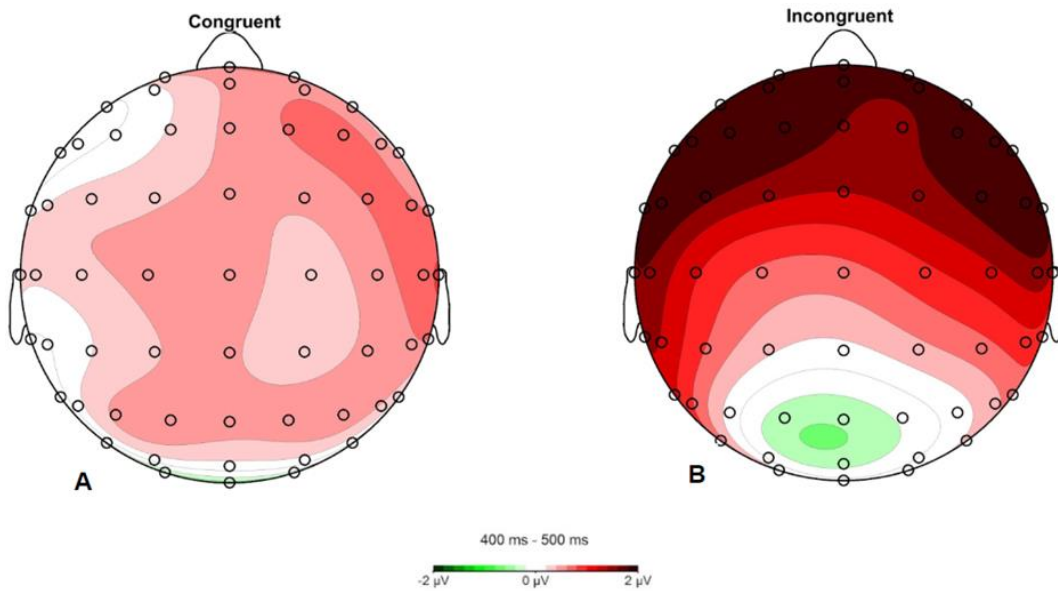


Figure 10: Scalp distribution of N400 activity for healthy participant “ctrl09”. The figure shows the topographical activities for the congruent (A) and incongruent (B) condition over the time interval of 400-500 ms. The color bar indicates the amplitudes of the peaks. Amplitude scales depicted are independent from amplitude scales for graphs with waveforms.

3.2.6 *Ctrl11*

The topographical maps in Figure 11b show more negative activity for the incongruent condition ($M=-3.69 \mu\text{V}$, $SD=2.45 \mu\text{V}$) mainly over the central and parietal areas, and also over the frontal area, skewed to the right hemisphere. Figure 11a shows the map for the congruent condition shows comparatively less negative activity ($M=-1.18 \mu\text{V}$, $SD=0.98 \mu\text{V}$) over the parietal and occipital regions, slightly skewed towards the right hemisphere. The peak of the congruent waveform was observed earlier ($M=531$, $SD=24.1\text{ms}$) than the incongruent waveform ($M=546\text{ms}$, $SD=26.5\text{ms}$).

The serial permutation t-test for the condition indicated a significant difference, as represented by the gray bars, between 400 and 500ms at the C3, and Cz electrodes, the mean of the 3 central electrodes (C3, Cz, C4), and the mean of the 6 central and parietal electrodes (C3, P3, Cz, Pz, C4, P4) (See Figure 21 in Appendix A).

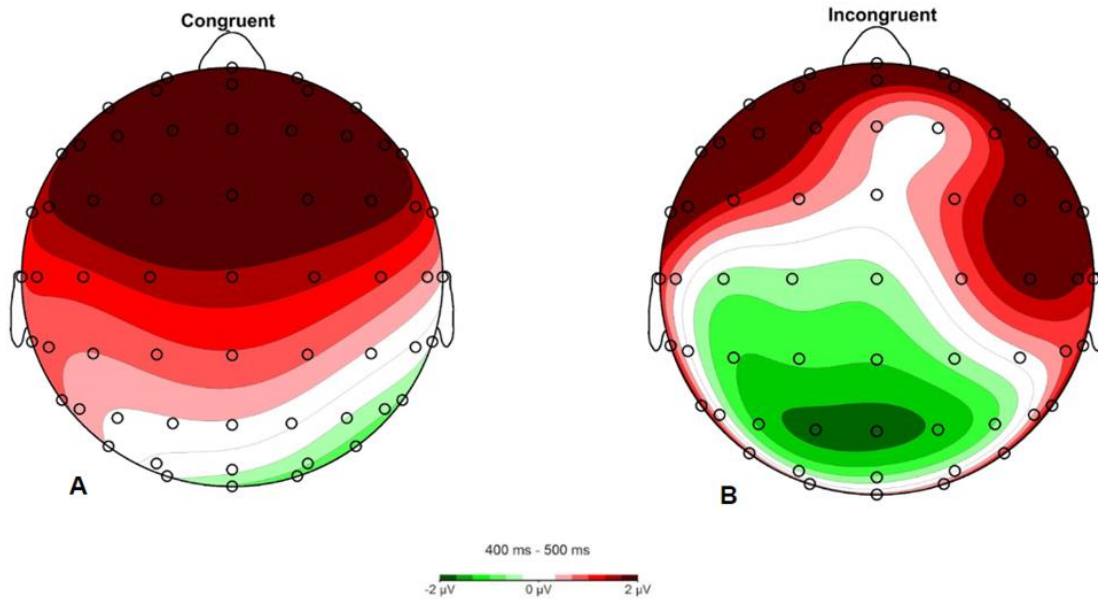


Figure 11: Scalp distribution of N400 activity for healthy participant “ctrl11”. The figure shows the topographical activities for the congruent (A) and incongruent (B) condition over the time interval of 400-500 ms. The color bar indicates the amplitudes of the peaks. Amplitude scales depicted are independent from amplitude scales for graphs with waveforms.

3.3 UWS Patient

Patient profile: The patient was a male aged 48 years, admitted for a traumatic brain injury from a fall down more than 12 stairs. This fall caused hemorrhaging in various regions of the brain including a right subdural and subarachnoid region of the cranium, and a right cerebellar hemorrhage multi-compartmental intracranial hemorrhage including right subacute subdural hemorrhage, bilateral subarachnoid hemorrhage at the basal cisterns, and a right cerebellar intracerebral hemorrhage.

Figure 12b shows more negative N400 activity over the frontal and central regions over the time interval of 500-700 ms. The scalp distribution for the congruent condition over this time interval indicates N400 activity over the left frontal and central regions (Figure 12a). The grand average of the trials indicates slightly delayed N400 activity, between 500 and 700ms (Figure 13). The amplitude of incongruent waveform appears to be more negative over the 3 frontal (F3, Fz, F4) and 3 central (C3, Cz, C4) electrodes, with little difference between the amplitudes for the congruent and incongruent condition over the parietal (P3, Pz, P4) electrodes. However, inferential statistical analysis showed that their response to incongruent condition ($M=-0.421 \mu\text{V}$, $SD=1.27 \mu\text{V}$) was less negative than the response to the congruent condition ($M=-1.36 \mu\text{V}$, $SD=0.959 \mu\text{V}$), with the incongruent peak appearing earlier ($M=466\text{ms}$, $SD=27.8\text{ms}$) than the congruent peak ($M=499\text{ms}$, $SD=35.3\text{ms}$).

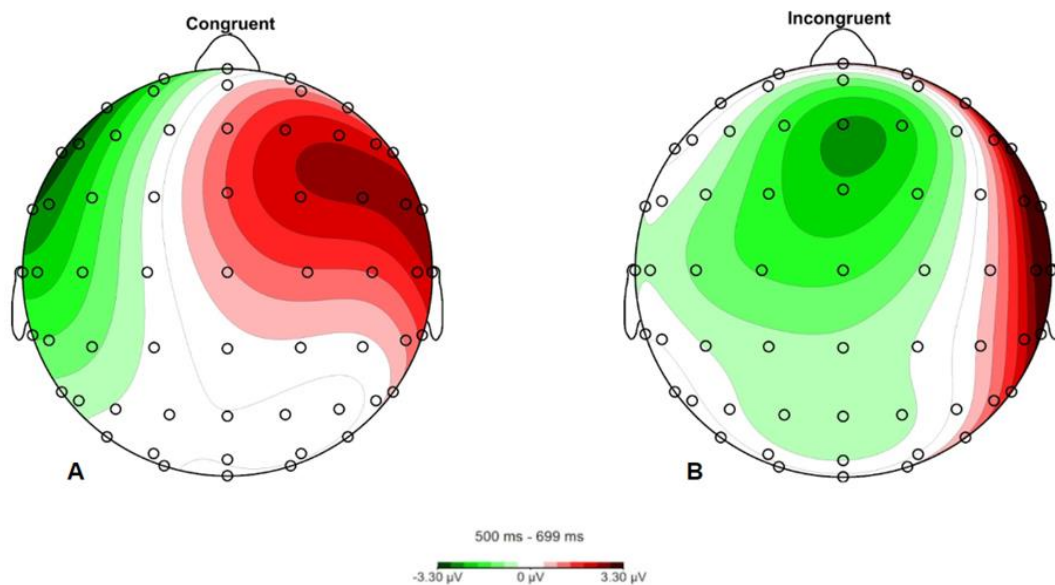


Figure 12: Scalp distribution of N400 activity over 350-600ms for a UWS patient. These figures show the topographical distribution of the N400 activity in response to A) congruent and B) incongruent condition. Amplitude scales depicted are independent from amplitude scales for graphs with waveforms.

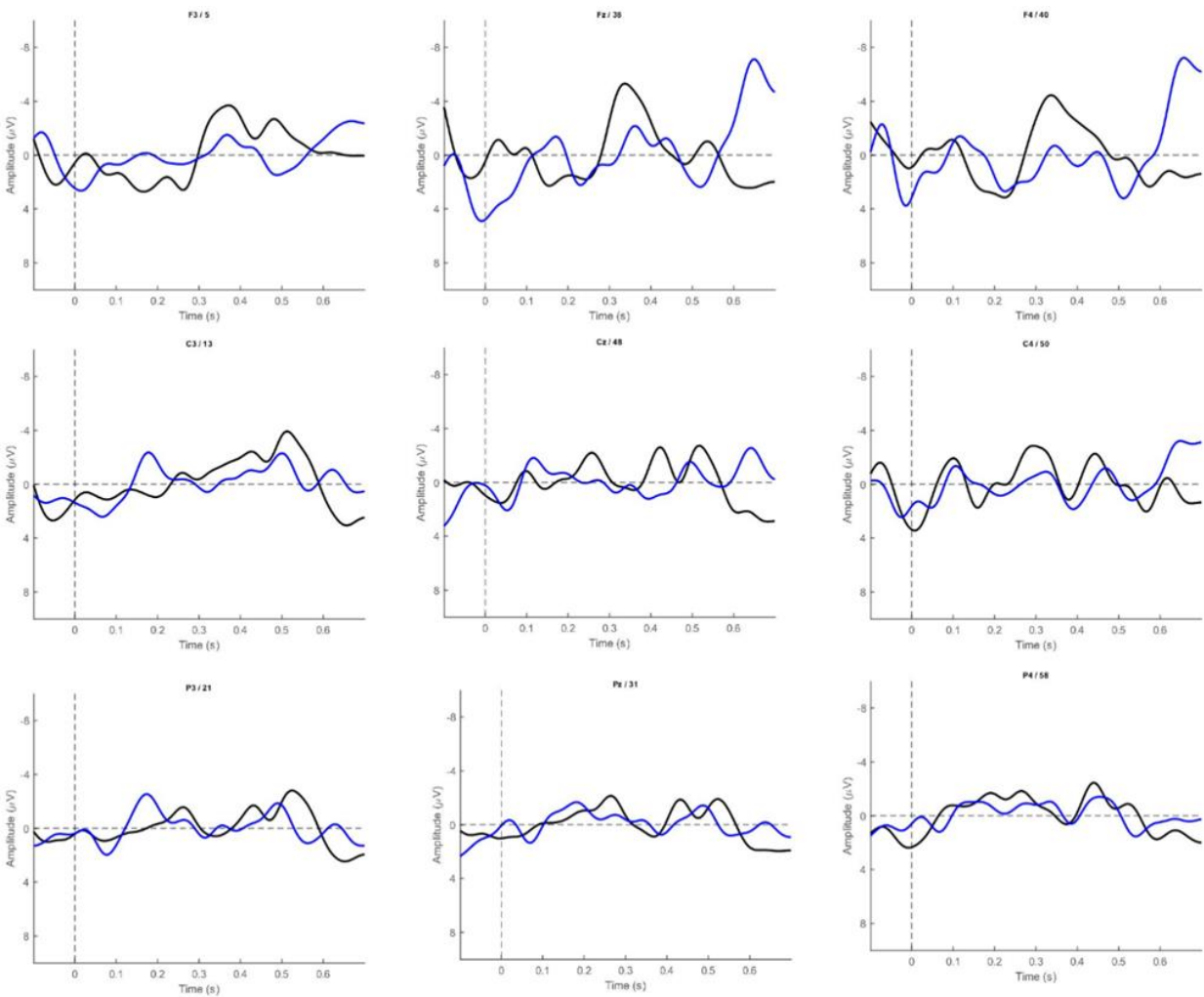


Figure 13: Graph depicting congruent (black) and incongruent (blue) waveforms over 3 frontal, 3 central and 3 parietal electrodes for a UWS patient. The congruent and incongruent waveforms are shown over a time epoch of -100 to 700 ms over the F3, Fz, F4, C3, Cz, C4, P3, Pz, & electrodes. Amplitude scales depicted are independent from amplitude scales for topographical maps.

4. Discussion

Traditional N400 paradigms with sentences as stimuli could be complex and taxing to the working memory in patients with neurological illnesses and damage. In this study, 18 healthy participants and one UWS patient were tested to investigate N400 activity in response to linguistic and non-linguistic stimulus pairs, specifically environmental sounds and spoken words. The overall aim was to incorporate this neurophysiological protocol into future projects targeting the prediction of coma emergence and eventual functional outcome. The N400 component has been known to reflect cognitive processes associated with comprehension of linguistic and conceptually meaningful stimuli. Here, the N400 activity detection was performed at a group level and single-subject level using three different methods: visual inspection of the averaged ERPs, serial permutation t-tests and mixed effects ANOVA. An additional case study of a patient in UWS, and the grand average of the activity over 9 electrodes has also been included for comparison of N400 activity to the healthy participants.

In this study, environmental sounds were presented as primes and spoken words were presented as targets in the singular auditory modality (adapted from Van Petten & Rheinfelder, 1995). Additionally, Ballas et al. (1987) noted that environmental sounds are produced by a real event and have meaning associated with it due to the connection with that event. Previous experiments with non-linguistic stimuli in priming experiments have demonstrated that prime stimuli can transfer specific meaning or concepts and could be linked to linguistic stimuli (Kutas & Ferdermier 2011). Van Petten and Rheinfelder were the first ones to identify that environmental sounds can prime

conceptually and semantically congruent and incongruent words. It has been previously reported that environmental sounds tend to be processed differently based on contextual cues, familiarity and frequency of occurrence.

Currently, there are no studies that have used priming paradigms with meaningful non-linguistic stimuli to assess N400 activity in coma patient population. Most of the widely recognized N400 studies have solely focused on using sentences and word pairs to elicit the N400 component (Kutas and Hillyard, 1987; Kutas & Federmeier, 2011; Connolly et al., 1995; Holcomb and Anderson, 1993). Individuals who are not fluent in the language or familiar with the accent and dialect of a language cannot accurately reflect complex cognitive activity associated with processing meaningful stimuli. Additionally, patients with severe brain damage may struggle with memory, recollection, and language comprehension, which can make it difficult for them to appropriately process and respond to linguistic stimuli (D'Arcy et al., 2005).

This was the first study to explore the efficacy of unimodal priming paradigm comprised of environmental sounds and spoken words in a priming paradigm in eliciting the N400 effect for clinical research application for coma patients. Specifically, this study aimed to observe if N400 activity can be elicited by stimuli not directly linked to language, in an effort to make it less difficult for these patients to complex linguistic stimuli to observe higher order cognitive activity associated with the N400.

4.1 N100 and P200 components

In addition to the N400 component, the N100 and P200 components were also observed in response to the congruent condition. The N100 and P200 components can be observed over the frontal, central and parietal electrodes on a group level.

Significant differences were found in between the congruent and incongruent conditions for the P200 component over the frontal and central electrodes in the grand average of 18 healthy subjects.

These observations were in accordance with previous findings that indicated that these components indicate early sensory activity, observed in response to auditory stimuli. ()

The N100 and P200 components can also be observed in all the individual subjects, however not as significant differences between the responses to the congruent and incongruent conditions. These components are seen as early sensory responses to auditory stimuli (Kutas and Ferdermier, 2011)

4.2 P3b component

Another positive going peak was observed apart from P200 between 300 and 400 ms in response to the congruent condition, which could be the P3b component (Figures 5 & 14). This component has been observed in response to rare and task-relevant stimuli, and memory storage (Sutton et al., 1965; Polich, 2007). Additionally, the presentation of this activity over the central and parietal electrodes is in conjunction with previous literature (Polich, 2007). This could be attributed to the updating of context

for the spoken word in association with the conceptual meaning of the sound, i.e, the conceptual association of the word and sound may be formed (Courchesne, Hillyard, & Courchesne, 1977). P3b activity has also been seen in response to stimuli that are overly cognitively demanding (KOK, 2001), and could be associated with memory retrieval (Polich 2007).

4.3 N400 Component

4.3.1 Group level analysis:

In Figures 4,5,15 &15, the semantic response, i.e., N400 in response to incongruent sound-word pairs was observed to be larger than to congruent pairs over the time epoch of 400-600ms.

Additionally, the scalp distribution of the N400 component is mainly over the centro-parietal regions, in accordance with previous findings (Kutas & Federmier, 2011; Van Petten & Rheinfelder,1995) explaining this activity's correlation with semantic memory storage and processing.

The N400 activity showed slight asymmetry to the right hemisphere, as can be seen from the topographical distribution for the incongruent condition. This lateral asymmetry was also observed by Van Petten and Rheinfelder (1995), who reported similar results in response to spoken words as targets.

Figures 5 and 14 also show N400 activity over the frontal electrodes, which has previously been observed in response to visually presented word pairs (McCauley et al.,

1979; Cummings et al., 2006). Frontal N400 activity has also been seen in response to non-linguistic stimuli in the form of picture sequences conveying a story, paired with contextually related or unrelated words (Sitnikova et al., 2008). Other studies reported N400 activity in response to the conceptual information associated with celebrity faces (Voss & Paller, 2006) and in response to meaningful geometric shapes (Voss & Paller, 2007). Overall, these previous findings indicate that frontal N400 activity is associated with conceptual priming of the stimuli, which can be observed from the findings in this study. Curran and colleagues have also reported that frontal N400s are correlated with cognitive processes associated with familiarity and recognition (Curran et al., 2016). Additionally, it has also been reported as a response to auditory stimuli (Kutas & Ferdermeier, 2011; Van Petten & Rheinfelder, 1995). Some studies also reported that frontal N400s have been associated with conceptual processing due to priming, not necessarily associated with familiarity (Bentin, McCarthy, and Wood, 1985; Kutas and Ferdermeier, 2011; Connolly, Phillips and Forbes, 1995).

The N400 peaks, particularly observed for the incongruent condition, began 400ms or earlier and were distributed over the time epoch of 350-600ms. This earlier presentation of the N400 peaks can be related to the auditory perception and processing stimuli and tended to last longer when compared to N400 activity in response to visual stimuli, as reported by Holcomb and Anderson (1993).

The presentation of the incongruent N400 components, associated with the N400 effect, were observed mainly over the central and parietal electrodes, in accordance with previous literature (Kutas and Ferdermier 2011, Van Petten & Rheinfelder 1995), and also over some of the frontal electrodes.

The serial permutation t-test applied on a within subjects' design yielded significant differences between the N400 component in response to conceptually congruent and incongruent sound-word pairs. Previous literature (Groppe et al., 2011a; Collinridge 2013) mentions the use of cluster based non-parametric permutation t-tests help resolve p-value correction or thresholding of significance values that occur with parametric tests like ANOVAs.

This non-parametric test was followed by a parametric test in the form of a within-subjects mixed effects ANOVA to corroborate these results, and to explore whether the significance was observed for the amplitude and latency when comparing the congruent and incongruent conditions. This parametric test supported the findings of the permutations t-test, with significant effects for the condition observed over various electrodes for the amplitude and latency, as elaborated above.

The vital feature of tests that assess neurological function should be sensitivity, especially to assess brain activity in patients with dysfunctional neurological states such as patients with DOC to determine if they will recover. Thus, it is essential that such tests are able to reliably assess brain activity on an individual level in healthy participants. This enables such protocols to be used on DOC patients to obtain reliable results (Naccache et al., 2016).

4.3.2 Single subject analysis

This study also aimed to investigate whether significant N400 activity could be observed in several of the healthy participants on an individual level, using serial permutation t-tests across the trials for individual participants. This testing was done in an effort to develop a viable protocol for individual assessment of DOC patients.

Out of the 18 healthy subjects, 6 subjects showed significant differences between the N400 activity in response to the congruent and incongruent condition. The significant activity varies across the 6 participants, with differences across the 9 electrodes.

Most of the participants show significant differences in N400 activity in response to the congruent and incongruent condition over 400ms and 600ms, mainly over the centro-parietal regions of the scalp, which aligns with the N400 activity pattern over the grand average of 18 participants and previous literature.

Out of the 6 participants, one participant showed an early N400 effect, between 300 and 400ms. This activity has been observed in previous studies that used environmental sounds as targets (Hendrickson et al., 2015). Observation of frontal N400 activity amongst individual participants is indicative of this cognitive process of recognition and recollection (Curran et al., 2016).

4.4 UWS Patient analysis

This is the first DOC patient to be tested with a N400 paradigm consisting of linguistic and non-linguistic stimuli.

The graph of the grand average from one UWS patient shows a more negative peak in response to the incongruent sound word pairs compared to the N400 peak in response to the congruent sound word pairs. This pattern of activity aligns with the significant centro-parietal N400 activity across the grand average of 18 healthy participants, and also across 6 individual participants.

4.5 Limitations & future directions:

One of the issues encountered was the variability in the N400 activity across the individual participants who showed significant differences between the congruent and incongruent conditions, possibly due to the subjective perception of the environmental sounds (Ballas et al., 1987). This issue could be resolved by using environmental sounds that are of uniform volume and high quality, created by the researcher or obtained from online high-quality sound files.

While significant N400 effects were observed in 6 participants out of the total of 18 participants on an individual level, showing promise for the development of viable protocol in DOC patients, this protocol needs be refined as explained above for obtaining reliable and accurate results from most of the sample.

Another rectifying measure that could be collecting and using environmental sounds each participant or patient is most accustomed to in their individual lives. This could be

especially useful for patients with neurological dysfunction who are unable to easily comprehend complex linguistic stimuli such as those in sentence paradigms.

The use of linguistic stimuli could be a barrier to obtaining robust N400 data from patients who are not native and fluent speakers of the language. Creating a N400 paradigm with environmental sounds as primes and targets could help with the collection of reliable N400 activity from patients regardless of their native languages.

Finally, one participant had dyslexia and two participants had a history of concussions, which may have affected the structure and distribution of the N400 peaks.

5. Conclusion

Neurological disorders like DOCs render patients unable to respond to their environment or indicate their sense of self-awareness making it difficult for clinicians to estimate the extent to which their cognitive and sensory function is impaired. The considerable reliance of consciousness assessment scales on external and often subjective signs of cognitive function has affected accuracy of the diagnoses and prognoses provided to these patients, affecting their chance at survival and receiving rehabilitative interventions. With the advent of sensitive neuroimaging methods such as EEG-ERPs, the possibility of thoroughly examining various sensory and cognitive functions in non-communicative populations has become more promising.

The present study offers insight into the potential utility of an EEG-ERP paradigm to investigate complex cognitive activity associated with processing meaning. Specifically, this paradigm uses relatively non-demanding stimuli in the form of environmental sounds to make it easier for patients with neurological dysfunction and diverse language background to respond to appropriately. The findings of this study indicating the N400 effect collected from the healthy participants indicate the possibility of this paradigm's utility to induce this complex cognitive activity in DOC patients. Future work should aim to explore whether similar significant results can be observed in a higher percentage of the healthy participant test pool, and how the paradigm can be adjusted to achieve this outcome. Furthermore, future work should also explore whether significant results can be seen in patients with DOCs and possibly other non-communicative patients with

conditions that alter their neurological functioning.

References

- Andrews, K., Murphy, L., Munday, R., & Littlewood, C. (1996). Misdiagnosis of the vegetative state: retrospective study in a rehabilitation unit. *BMJ (Clinical Research Ed.)*, *313*(7048), 13–16. <https://doi.org/10.1136/bmj.313.7048.13>
- Armanfard, N., Komeili, M., Reilly, J. P., & Connolly, J. F. (2019). A Machine Learning Framework for Automatic and Continuous MMN Detection With Preliminary Results for Coma Outcome Prediction. *IEEE Journal of Biomedical and Health Informatics*, *23*(4), 1794–1804. <https://doi.org/10.1109/jbhi.2018.2877738>
- Balconi, M., & Arangio, R. (2015). The Relationship Between Coma Near Coma, Disability Ratings, and Event-Related Potentials in Patients with Disorders of Consciousness: A Semantic Association Task. *Applied Psychophysiology and Biofeedback*, *40*(4), 327–337. <https://doi.org/10.1007/s10484-015-9304-y>
- Balconi, M., Arangio, R., & Guarnerio, C. (2013). Disorders of Consciousness and N400 ERP Measures in Response to a Semantic Task. *The Journal of Neuropsychiatry and Clinical Neurosciences*, *25*(3), 237–243. <https://doi.org/10.1176/appi.neuropsych.12090227>
- Ballas, J. A., & Howard, J. H. (1987). Interpreting the Language of Environmental Sounds. *Environment and Behavior*, *19*(1), 91–114. <https://doi.org/10.1177/0013916587191005>

- Bentin, S., McCarthy, G., & Wood, C. C. (1985). Event-related potentials, lexical decision and semantic priming. *Electroencephalography and Clinical Neurophysiology*, 60(4), 343–355. [https://doi.org/10.1016/0013-4694\(85\)90008-2](https://doi.org/10.1016/0013-4694(85)90008-2)
- Boris, B., Daltrozzo, J., Norma, N., Mutschler, V., Lutun, P., Birbaumer, N., & Jaeger, A. (2005). Semantic processing in a coma patient. *Grand Rounds*, 37–41. <https://doi.org/10.1102/1470-5206.2005.0013>
- Collingridge, D. S. (2012). A Primer on Quantitized Data Analysis and Permutation Testing. *Journal of Mixed Methods Research*, 7(1), 81–97. <https://doi.org/10.1177/1558689812454457>
- Connolly, J. F., Byrne, J. M., & Dywan, C. A. (1995). Assessing adult receptive vocabulary with event-related potentials: An investigation of cross-modal and cross-form priming. *Journal of Clinical and Experimental Neuropsychology*, 17(4), 548–565. <https://doi.org/10.1080/01688639508405145>
- Connolly, J. F., Phillips, N. A., & Forbes, K. A. K. (1995). The effects of phonological and semantic features of sentence-ending words on visual event-related brain potentials. *Electroencephalography and Clinical Neurophysiology*, 94(4), 276–287. [https://doi.org/10.1016/0013-4694\(95\)98479-r](https://doi.org/10.1016/0013-4694(95)98479-r)
- Courchesne, E., Hillyard, S. A., & Courchesne, R. Y. (1977). P3 Waves to the Discrimination of Targets in Homogeneous and Heterogeneous Stimulus Sequences. *Psychophysiology*, 14(6), 590–597. <https://doi.org/10.1111/j.1469-8986.1977.tb01206.x>

- Cummings, A., Čeponienė, R., Koyama, A., Saygin, A. P., Townsend, J., & Dick, F. (2006). Auditory semantic networks for words and natural sounds. *Brain Research*, 1115(1), 92–107. <https://doi.org/10.1016/j.brainres.2006.07.050>
- D’Arcy, R. C. N., Connolly, J. F., & Eskes, G. A. (2000). Evaluation of reading comprehension with neuropsychological and event-related brain potential (ERP) methods. *Journal of the International Neuropsychological Society*, 6(5), 556–567. <https://doi.org/10.1017/s1355617700655054>
- D’Arcy, R. C. N., Connolly, J. F., Service, E., Hawco, C. S., & Houlihan, M. E. (2004). Separating phonological and semantic processing in auditory sentence processing: A high-resolution event-related brain potential study. *Human Brain Mapping*, 22(1), 40–51. <https://doi.org/10.1002/hbm.20008>
- D’Arcy, R. C. N., Service, E., Connolly, J. F., & Hawco, C. S. (2005). The influence of increased working memory load on semantic neural systems: a high-resolution event-related brain potential study. *Cognitive Brain Research*, 22(2), 177–191. <https://doi.org/10.1016/j.cogbrainres.2004.08.007>
- Daltrozzo, J., Wioland, N., Mutschler, V., Lutun, P., Calon, B., Meyer, A., Pottecher, T., Lang, S., Jaeger, A., & Kotchoubey, B. (2009). Cortical Information Processing in Coma. *Cognitive and Behavioral Neurology*, 22(1), 53–62. <https://doi.org/10.1097/wnn.0b013e318192ccc8>
- de Cheveigne, A., & Nelken, I. (2019). Filters: When, Why, and How (Not) to Use Them. *Neuron*, 102(2), 280–293. <https://doi.org/10.1016/j.neuron.2019.02.039>

- Duncan, C. C., Barry, R. J., Connolly, J. F., Fischer, C., Michie, P. T., Näätänen, R., Polich, J., Reinvang, I., & Van Petten, C. (2009). Event-related potentials in clinical research: Guidelines for eliciting, recording, and quantifying mismatch negativity, P300, and N400. *Clinical Neurophysiology*, *120*(11), 1883–1908. <https://doi.org/10.1016/j.clinph.2009.07.045>
- Fischer, C., Dailler, F., & Morlet, D. (2008). Novelty P3 elicited by the subject's own name in comatose patients. *Clinical Neurophysiology*, *119*(10), 2224–2230. <https://doi.org/10.1016/j.clinph.2008.03.035>
- Fischer, C., Morlet, D., Bouchet, P., Luaute, J., Jourdan, C., & Salord, F. (1999). Mismatch negativity and late auditory evoked potentials in comatose patients. *Clinical Neurophysiology*, *110*(9), 1601–1610. [https://doi.org/10.1016/s1388-2457\(99\)00131-5](https://doi.org/10.1016/s1388-2457(99)00131-5)
- Gawryluk, J. R., D'Arcy, R. C., Connolly, J. F., & Weaver, D. F. (2010). Improving the clinical assessment of consciousness with advances in electrophysiological and neuroimaging techniques. *BMC Neurology*, *10*, 11. <https://doi.org/10.1186/1471-2377-10-11>
- Giacino, J. T., Fins, J. J., Laureys, S., & Schiff, N. D. (2014). Disorders of consciousness after acquired brain injury: the state of the science. *Nature Reviews Neurology*, *10*(2), 99–114. <https://doi.org/10.1038/nrneurol.2013.279>
- Gosseries, O., Di, H., Laureys, S., & Boly, M. (2014). Measuring Consciousness in Severely Damaged Brains. *Annual Review of Neuroscience*, *37*(1), 457–478. <https://doi.org/10.1146/annurev-neuro-062012-170339>

- Hendrickson, K., Walenski, M., Friend, M., & Love, T. (2015). The organization of words and environmental sounds in memory. *Neuropsychologia*, *69*, 67–76.
<https://doi.org/10.1016/j.neuropsychologia.2015.01.035>
- Holcomb, P. J., & Anderson, J. E. (1993). Cross-modal semantic priming: A time-course analysis using event-related brain potentials. *Language and Cognitive Processes*, *8*(4), 379–411. <https://doi.org/10.1080/01690969308407583>
- Holeckova, I., Fischer, C., Morlet, D., Delpuech, C., Costes, N., & Mauguière, F. (2008). Subject's own name as a novel in a MMN design: A combined ERP and PET study. *Brain Research*, *1189*, 152–165.
<https://doi.org/10.1016/j.brainres.2007.10.091>
- Koelsch, S., Kasper, E., Sammler, D., Schulze, K., Gunter, T., & Friederici, A. D. (2004). Music, language and meaning: brain signatures of semantic processing. *Nature Neuroscience*, *7*(3), 302–307. <https://doi.org/10.1038/nn1197>
- Kok, A. (2001). On the utility of P3 amplitude as a measure of processing capacity. *Psychophysiology*, *38*(3), 557–577. <https://doi.org/10.1017/s0048577201990559>
- Kutas, M., & Federmeier, K. D. (2011). Thirty Years and Counting: Finding Meaning in the N400 Component of the Event-Related Brain Potential (ERP). *Annual Review of Psychology*, *62*(1), 621–647.
<https://doi.org/10.1146/annurev.psych.093008.131123>
- Laureys, S., Celesia, G. G., Cohadon, F., Lavrijsen, J., León-Carrión, J., Sannita, W. G., Sazbon, L., Schmutzhard, E., von Wild, K. R., Zeman, A., & Dolce, G. (2010).

- Unresponsive wakefulness syndrome: a new name for the vegetative state or apallic syndrome. *BMC Medicine*, 8(1). <https://doi.org/10.1186/1741-7015-8-68>
- Leckey, M., & Federmeier, K. D. (2019). The P3b and P600(s): Positive contributions to language comprehension. *Psychophysiology*, e13351. <https://doi.org/10.1111/psyp.13351>
- Morlet, D., & Fischer, C. (2013). MMN and Novelty P3 in Coma and Other Altered States of Consciousness: A Review. *Brain Topography*, 27(4), 467–479. <https://doi.org/10.1007/s10548-013-0335-5>
- Naccache, L., Marti, S., Sitt, J. D., Trübutschek, D., & Berkovitch, L. (2016). Why the P3b is still a plausible correlate of conscious access? A commentary on Silverstein et al., 2015. *Cortex*, 85, 126–128. <https://doi.org/10.1016/j.cortex.2016.04.003>
- Naccache, L., Puybasset, L., Gaillard, R., Serve, E., & Willer, J.-C. (2005). Auditory mismatch negativity is a good predictor of awakening in comatose patients: a fast and reliable procedure. *Clinical Neurophysiology*, 116(4), 988–989. <https://doi.org/10.1016/j.clinph.2004.10.009>
- Orgs, G., Lange, K., Dombrowski, J., & Heil, M. (2007). Is conceptual priming for environmental sounds obligatory? *International Journal of Psychophysiology*, 65(2), 162–166. <https://doi.org/10.1016/j.ijpsycho.2007.03.003>
- Polich, J. (2007). Updating P300: an integrative theory of P3a and P3b. *Clinical Neurophysiology : Official Journal of the International Federation of Clinical*

Neurophysiology, 118(10), 2128–2148.

<https://doi.org/10.1016/j.clinph.2007.04.019>

Rämä, P., Relander-Syrjänen, K., Öhman, J., Laakso, A., Näätänen, R., & Kujala, T. (2010). Semantic processing in comatose patients with intact temporal lobes as reflected by the N400 event-related potential. *Neuroscience Letters*, 474(2), 88–92. <https://doi.org/10.1016/j.neulet.2010.03.012>

Schnakers, C., Vanhaudenhuyse, A., Giacino, J., Ventura, M., Boly, M., Majerus, S., Moonen, G., & Laureys, S. (2009). Diagnostic accuracy of the vegetative and minimally conscious state: Clinical consensus versus standardized neurobehavioral assessment. *BMC Neurology*, 9(1). <https://doi.org/10.1186/1471-2377-9-35>

Seel, R. T., Sherer, M., Whyte, J., Katz, D. I., Giacino, J. T., Rosenbaum, A. M., Hammond, F. M., Kalmar, K., Pape, T. L.-B., Zafonte, R., Biester, R. C., Kaelin, D., Kean, J., & Zasler, N. (2010). Assessment scales for disorders of consciousness: Evidence-based recommendations for Clinical Practice and Research. *Archives of Physical Medicine and Rehabilitation*, 91(12), 1795–1813. <https://doi.org/10.1016/j.apmr.2010.07.218>

Sitnikova T, Holcomb PJ, Kiyonaga KA, Kuperberg GR. Two neurocognitive mechanisms of semantic integration during the comprehension of visual real-world events. *J Cogn Neurosci*. 2008;20:1–21.

- Sperber, R. D., McCauley, C., Ragain, R. D., & Weil, C. M. (1979). Semantic priming effects on picture and word processing. *Memory & Cognition*, 7(5), 339–345. <https://doi.org/10.3758/bf03196937>
- Stróžak, P., Abedzadeh, D., & Curran, T. (2016). Separating the FN400 and N400 potentials across recognition memory experiments. *Brain Research*, 1635, 41–60. <https://doi.org/10.1016/j.brainres.2016.01.015>
- Sutton S, Braren M, Zubin J, et al. Evoked potential correlates of stimulus uncertainty. *Science*. 1965;150:1187–1188.
- VanPetten, C., & Rieffers, H. (1995). Conceptual relationships between spoken words and environmental sounds: Event-related brain potential measures. *Neuropsychologia*, 33(4), 485–508. [https://doi.org/10.1016/0028-3932\(94\)00133-a](https://doi.org/10.1016/0028-3932(94)00133-a)
- Wannez, S., Heine, L., Thonnard, M., Gosseries, O., & Laureys, S. (2017). The repetition of behavioral assessments in diagnosis of disorders of consciousness. *Annals of Neurology*, 81(6), 883–889. <https://doi.org/10.1002/ana.24962>

Appendices

Appendix A: Graphs of waveforms from healthy participants

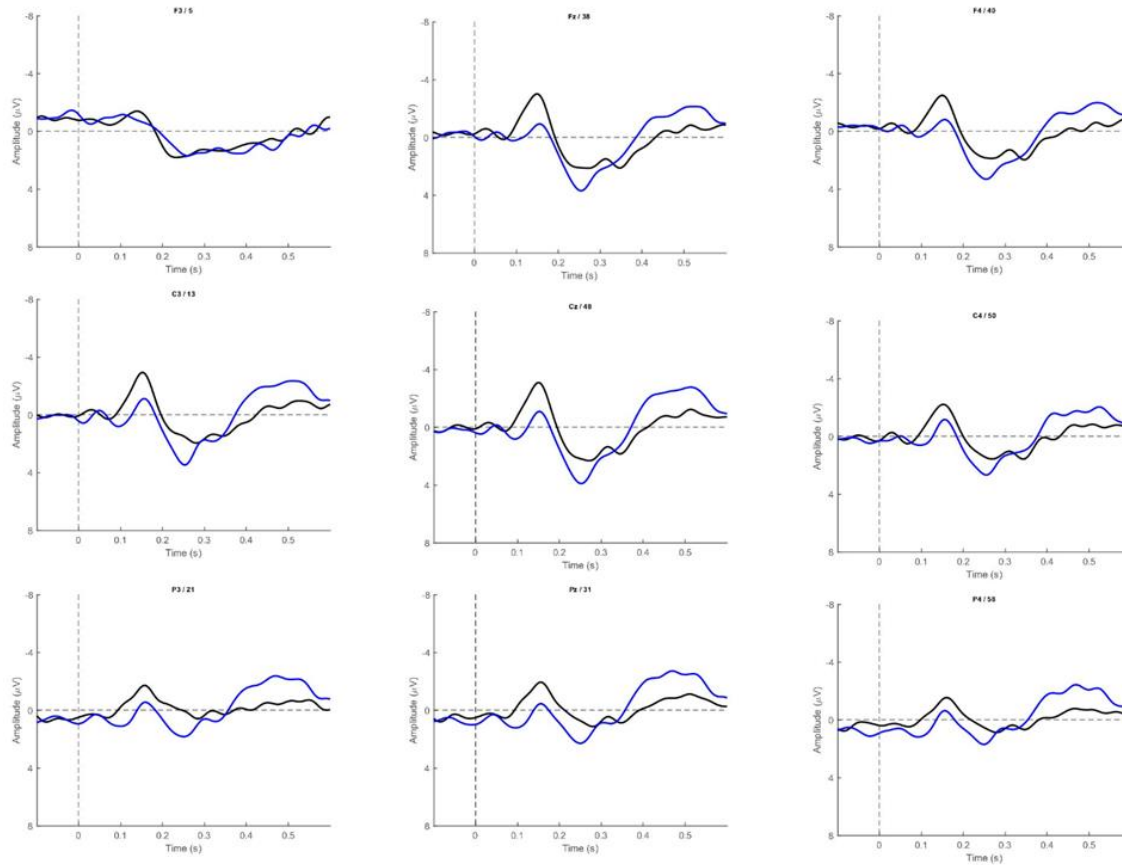


Figure 14: Graphs depicting congruent (black) and incongruent (blue) waveforms over 3 frontal, 3 central and 3 parietal electrodes of the grand average of 18 healthy participants. The congruent and incongruent waveforms are shown over a time epoch of -100 to 700 ms over the F3, Fz, F4, C3, Cz, C4, P3, Pz, & electrodes.

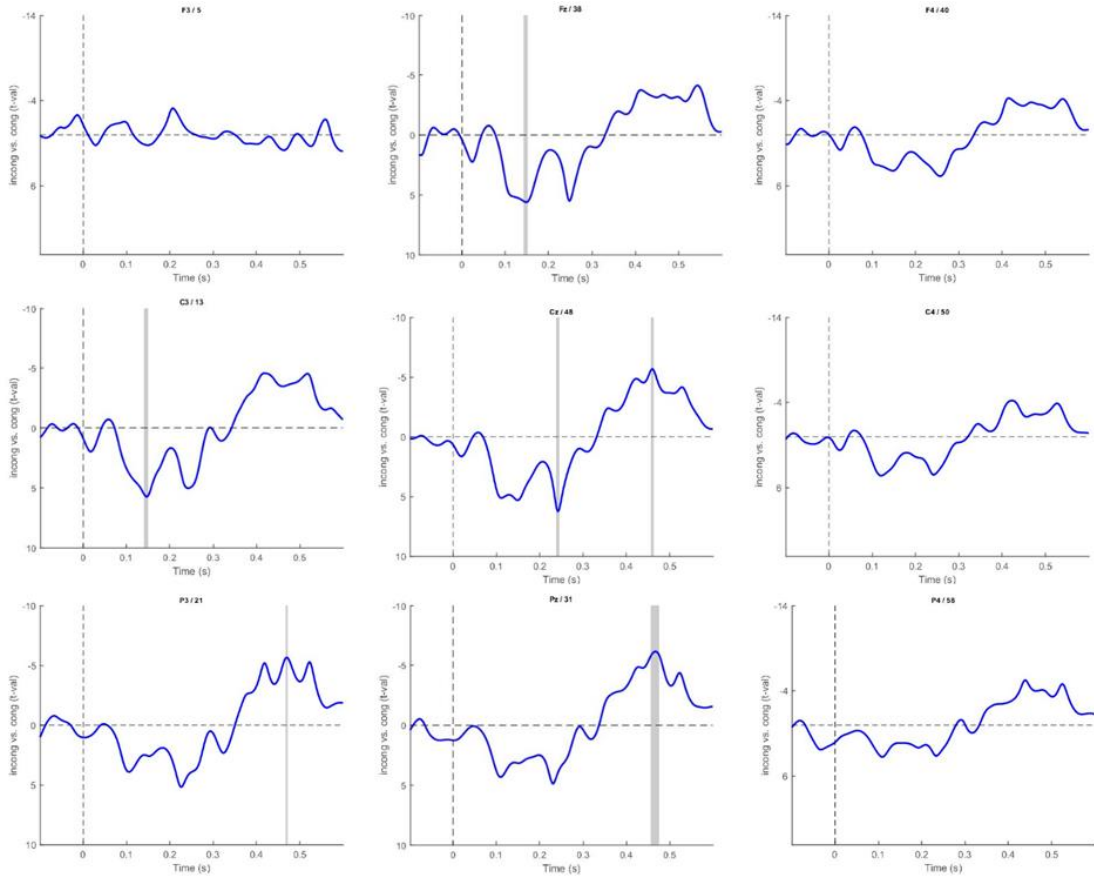


Figure 15: Graphs depicting differences between the t -values for the congruent and incongruent condition reliably detected by permutations t -test ($p < 0.05$) of the grand average of 18 healthy participants. Significant intervals are denoted by the gray areas.

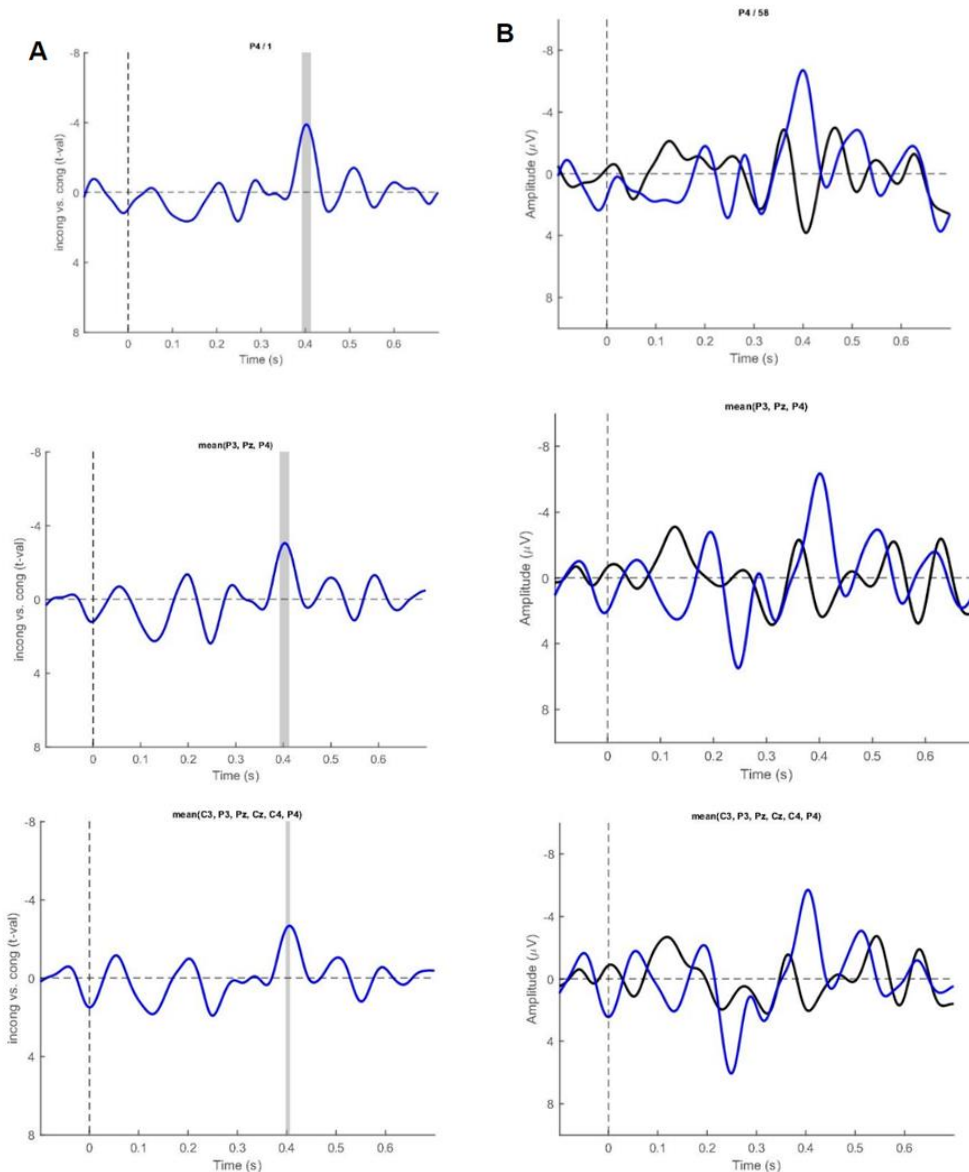
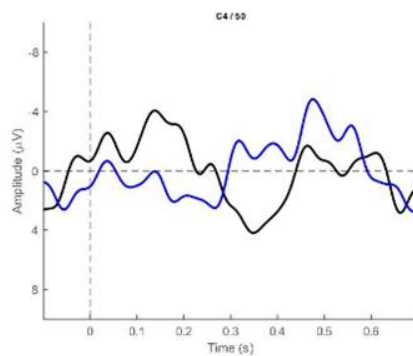
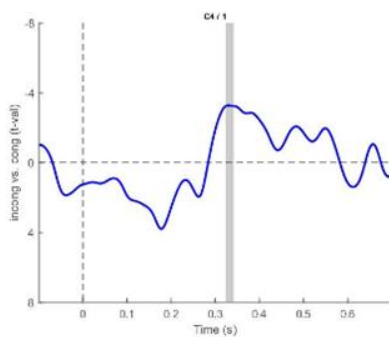
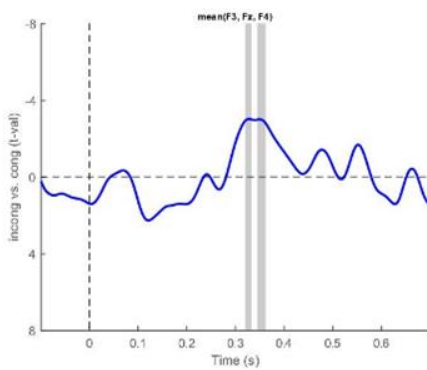
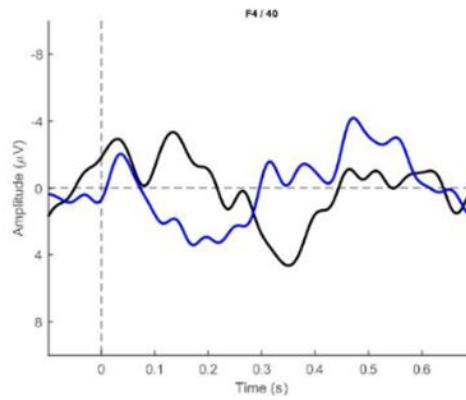
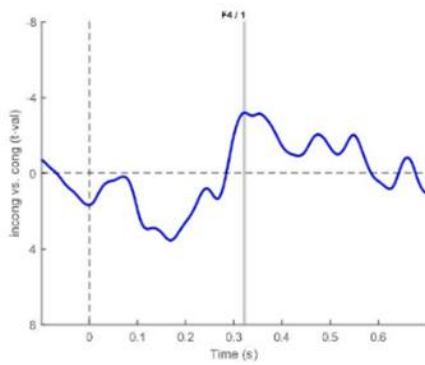
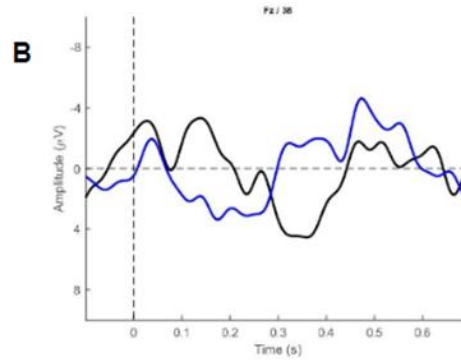
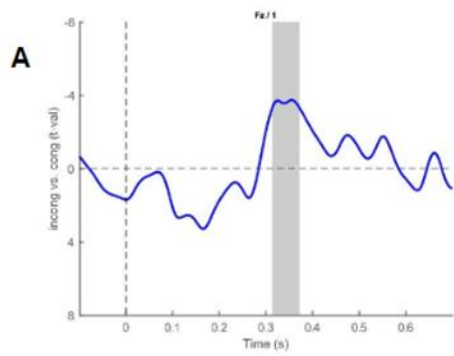


Figure 16: Graphs of the ERPs in 'pilot01' over the P4, mean of the 3 parietal (P3, Pz, P4) and mean of the 6 centro-parietal (C3, P3, Cz, Pz, C4, P4) electrodes. A) Grand averaged waveforms for the congruent condition represented by the black waveform, and the incongruent condition, represented by the blue waveform. B) Difference between the t-values for the congruent and incongruent condition reliably detected by permutations t-test ($p < 0.05$). Significant intervals are denoted by the gray areas.



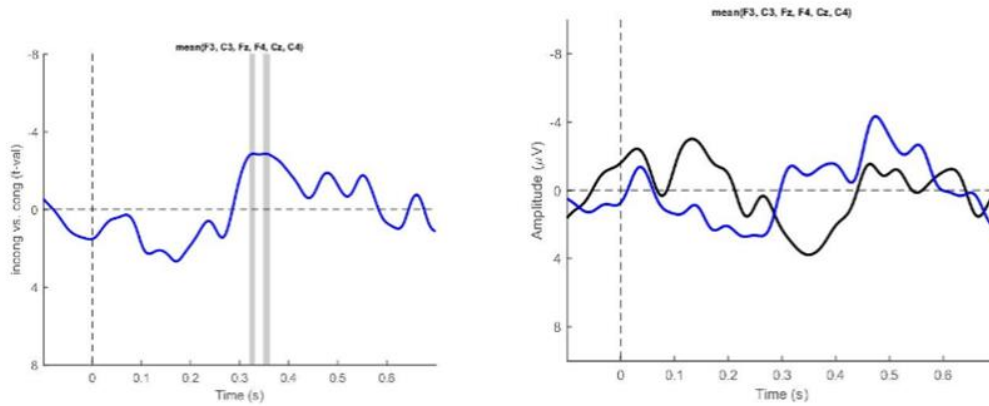


Figure 17: Graphs of the ERPs in 'pilot09' over the Fz, F4, mean of the 3 frontal (F3, Fz, F4), C4, and mean of the 6 fronto-central (F3, C3, Fz, Cz, F4, C4) electrodes. A) Grand averaged waveforms for the congruent condition represented by the black waveform, and the incongruent condition, represented by the blue waveform. B) Difference between the t-values for the congruent and incongruent condition reliably detected by permutations t-test ($p < 0.05$). Significant intervals are denoted by the gray areas.

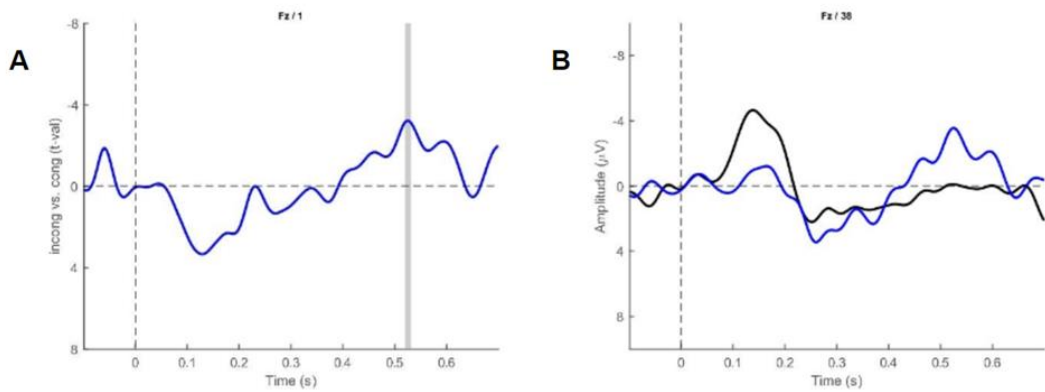
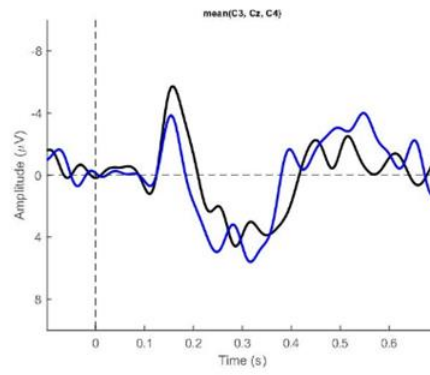
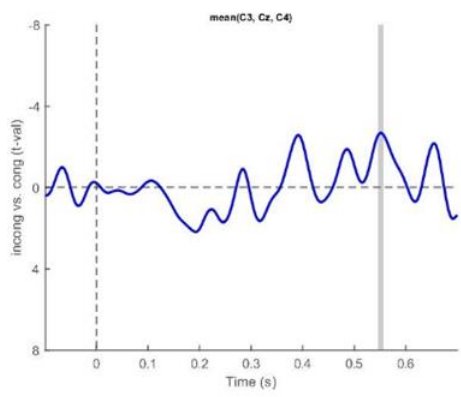
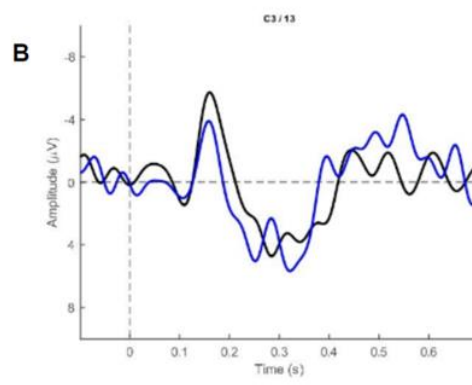
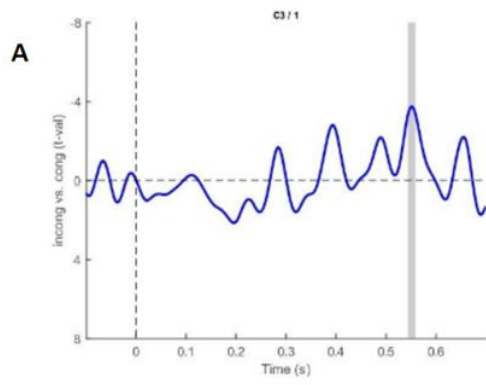


Figure 18: Graphs of the ERPs in 'pilot10' over the Fz electrode. A) Grand averaged waveforms for the congruent condition represented by the black waveform, and the incongruent condition, represented by the blue waveform. B) Difference between the t-values for the congruent and incongruent condition reliably detected by permutations t-test ($p < 0.05$). Significant intervals are denoted by the gray areas.



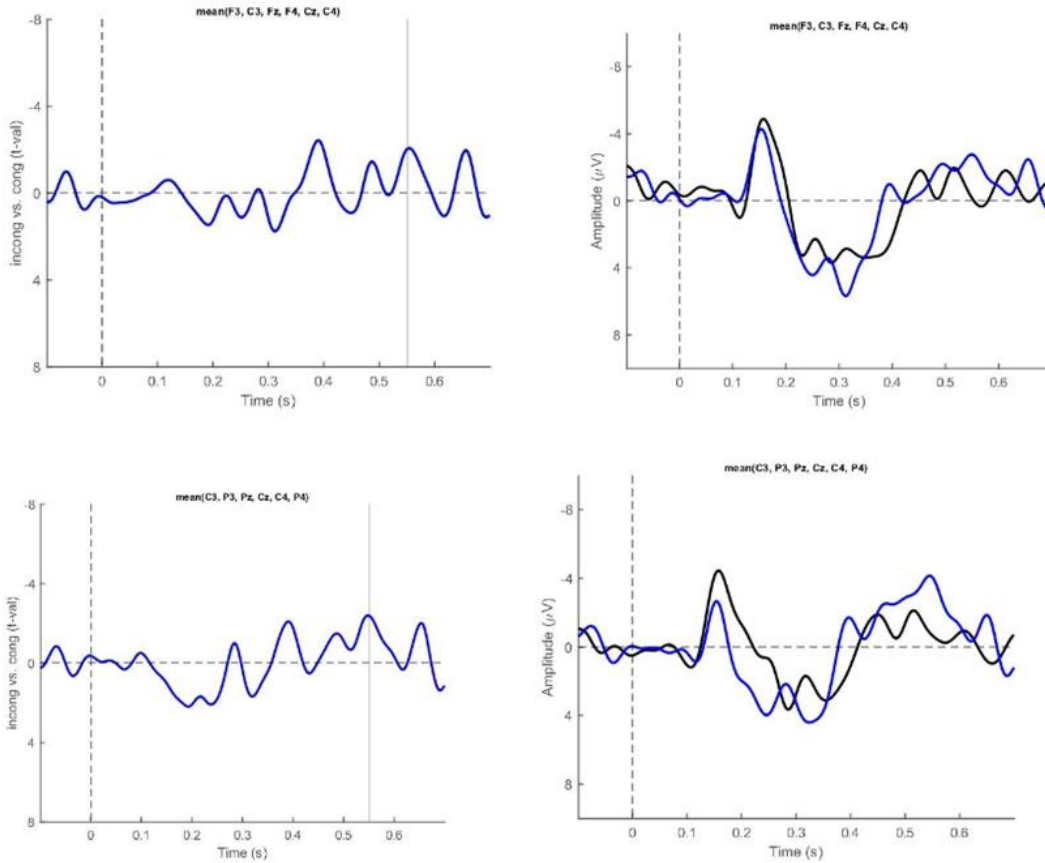


Figure 19: Graphs of the ERPs in 'ctrl04' over the C3, mean of the 3 central (C3, Cz, C4), mean of the 6 fronto-central (F3, C3, Fz, Cz, F4, C4) and mean of the 6 centro-parietal (C3, P3, Cz, Pz, C4, P4) electrodes. A) Grand averaged waveforms for the congruent condition represented by the black waveform, and the incongruent condition, represented by the blue waveform. B) Difference between the t-values for the congruent and incongruent condition reliably detected by permutations t-test ($p < 0.05$). Significant intervals are denoted by the gray areas.

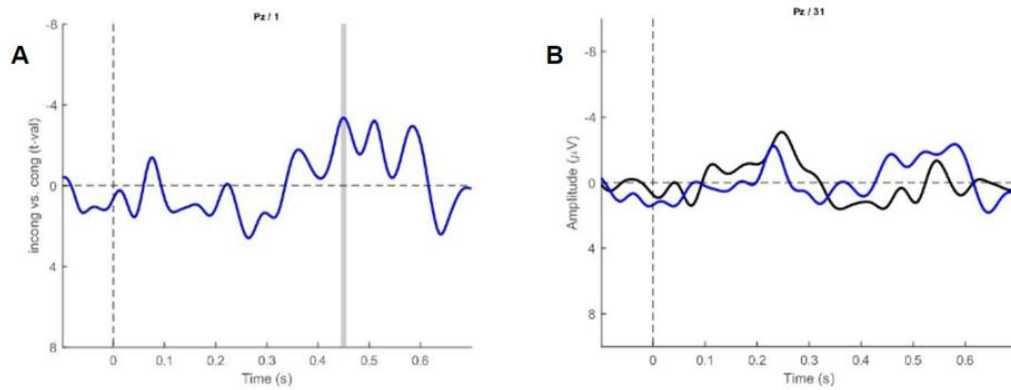


Figure 20: Graphs of the ERPs in 'ctrl09' over the Pz electrode. A) Grand averaged waveforms for the congruent condition represented by the black waveform, and the incongruent condition, represented by the blue waveform. B) Difference between the t-values for the congruent and incongruent condition reliably detected by permutations t-test ($p < 0.05$). Significant intervals are denoted by the gray areas.

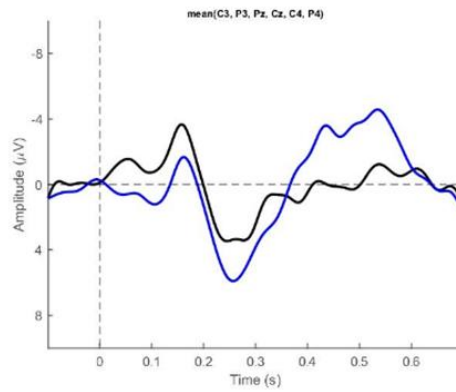
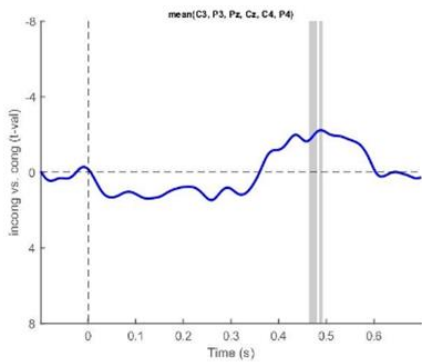
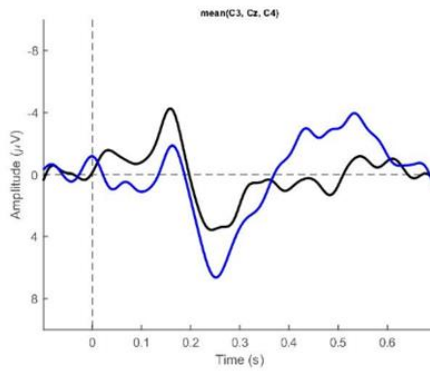
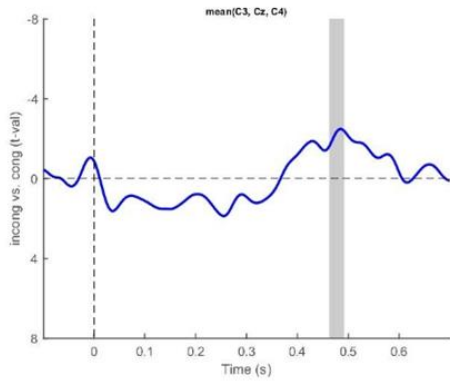
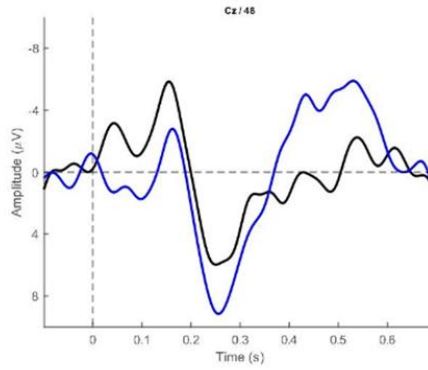
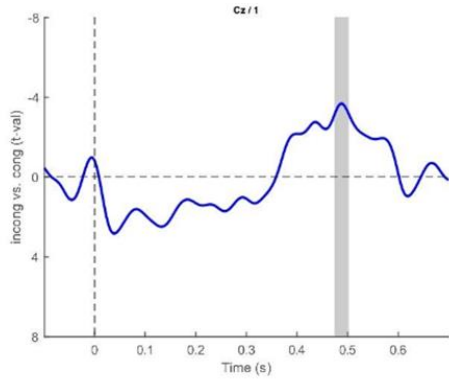
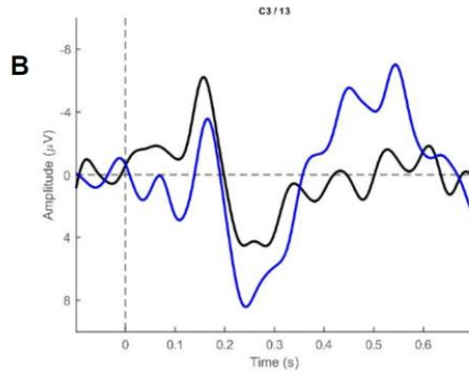
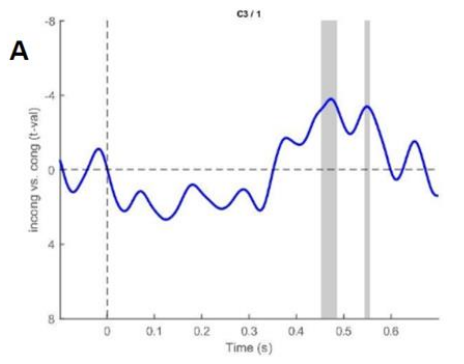


Figure 21: *Graphs of the ERPs in 'ctrl11' over the C3, Cz, mean of 3 central (C3, Cz, C4) and mean of the 6 fronto-central (F3, C3, Fz, Cz, F4, C4) electrodes. A) Grand averaged waveforms for the congruent condition represented by the black waveform, and the incongruent condition, represented by the blue waveform. B) Difference between the t-values for the congruent and incongruent condition reliably detected by permutations t-test ($p < 0.05$). Significant intervals are denoted by the gray areas.*